View metadata, citation and similar papers at core.ac.uk
brought to you by CORE
provided by Elsevier - Publisher Connector

Gene expression changes in the human diaphragm after cardiothoracic surgery

Tseng-Tien Huang, PhD,[a] Harsha V. Deoghare, PhD,[a] Barbara K. Smith, PhD,[a] Thomas M. Beaver, MD,[b] Henry V. Baker, PhD,[c] Alvine C. Mehinto, PhD,[d] and A. Daniel Martin, PhD, PT[a]

Objective: We examined the effects of cardiothoracic surgery, including cardiopulmonary bypass and controlled mechanical ventilation, on messenger RNA gene expression in human diaphragm. We hypothesized that genes responsible for stress response, redox regulation, protein turnover, energy metabolism, and contractile function would be altered by cardiothoracic surgery.

Methods: Paired diaphragm biopsy samples were obtained from 5 male patients (67 ± 11 years) during cardiothoracic surgery, the first as soon as the diaphragm was exposed and the second as late in surgery as possible (4.9 ± 1.8 hours between samples). We profiled messenger RNA from 5 specimen pairs with microarray analysis (Hu U133 plus 2.0; Affymetrix UK Ltd, High Wycombe, UK). Quantitative reverse transcriptase polymerase chain reaction was performed with a select set of genes exhibiting differential expression for validation.

Results: Microarray analysis identified 779 differentially expressed (early vs late samples) unique gene products ($P < .005$). Postoperatively, genes related to stress response and redox regulation were upregulated. Additionally, we found significantly upregulated expression of cathepsin C (2.7-fold), cathepsin L1 (2.0-fold), various ubiquitin-conjugating enzymes (E2, approximately 1.8-fold), proinflammatory cytokine interleukin 6 (15.6-fold), and muscle-specific ubiquitin ligase (MuRF-1, 2.6-fold). Comparison of fold change values obtained by quantitative reverse transcriptase polymerase chain reaction and microarray yielded significant correlation ($r = 0.95$, $P < .0001$).

Conclusions: Cardiothoracic surgery results in rapid changes in human diaphragm gene expression in the operating room, including genes related to stress response, inflammation, redox regulation, and proteolysis. These results may provide insight into diaphragm muscle biology after prolonged cardiothoracic procedures. (J Thorac Cardiovasc Surg 2011;142:1214-22)

ET/BS

Supplemental material is available online.

After cardiothoracic surgery (CTS), approximately 10% of patients require prolonged mechanical ventilation (MV, support needed for at least 48 hours after surgery), and more than 40% in-hospital mortality has been reported in this population.[1] Although the mechanisms responsible for the need for prolonged MV have not been fully elucidated, accumulating evidence links prolonged MV with inspiratory muscle dysfunction.[2] Animal studies have shown that MV use itself leads to a rapid, time-dependent decrease in diaphragmatic contractility.[3] DeRuisseau and colleagues[4] examined diaphragm gene expression after 6 to 18 hours of controlled MV in rats and found significant upregulation of genes related to cell growth and maintenance, stress response, and nucleic acid metabolism, with concomitant downregulation in the structural protein and energy metabolism categories. In contrast, preservation of diaphragm activity with assisted MV modes[5] or short periods of spontaneous respiration[6] lessens contractile dysfunction in animals supported with MV. In human studies, Levine and associates[7] showed clinically significant diaphragm muscle atrophy after as little as 18 to 69 hours of controlled MV, which is consistent with the changes seen in the animal models.

In addition to MV itself, other factors during CTS may also influence diaphragm function, such as the use of cardiopulmonary bypass (CPB),[8] hypothermia,[9] and neuromuscular blockade.[10] Data suggest that these factors can affect diaphragm contractile properties or neuromuscular transmission alone or in combination with the use of controlled MV. Ermilov and coworkers[8] found that a 1-hour exposure to CPB followed by a 90-minute recovery period resulted in an approximately 25% decline in diaphragm-specific force

From the Departments of Physical Therapy,[a] Surgery,[b] Molecular Genetics and Microbiology,[c] and Physiological Sciences,[d] University of Florida, Gainesville, Fla.
Supported by National Institutes of Health grant T32 HD043730 and a Foundation for Physical Therapy Promotion of Doctoral Studies Scholarship (to B.K.S.).
Disclosures: Authors have nothing to disclose with regard to commercial support.
Received for publication Dec 8, 2010; revisions received Feb 7, 2011; accepted for publication Feb 22, 2011; available ahead of print April 4, 2011.
Address for reprints: A. Daniel Martin, PhD, PT, PO Box 100154, Gainesville, FL 32610-0154 (E-mail: dmartin@phhp.ufl.edu).
0022-5223/$36.00
Copyright © 2011 by The American Association for Thoracic Surgery
doi:10.1016/j.jtcvs.2011.02.025

Abbreviations and Acronyms

CPB	= cardiopulmonary bypass
CTS	= cardiothoracic surgery
IL	= interleukin
JAK-STAT	= janus kinase/signal transducers and activators of transcription
MV	= mechanical ventilation

capacity and impaired neuromuscular transmission relative to time-matched rats supported with MV without CBP. During CPB, the expressions of proinflammatory cytokines such as interleukin (IL) 6 and IL-8 surge in respiratory muscle,[11] and elevated levels of these cytokines have been associated with diaphragm contractile dysfunction.[8] These findings suggest that the stressor of CTS may alter diaphragm function very rapidly and that cytokine expression could contribute to diaphragm dysfunction. It is unknown, however, whether or how rapidly messenger RNA gene expression in the human diaphragm is altered by CTS.

The objective of this study was therefore to examine the effects of CTS, which include the use of controlled MV in combination with the use of CPB, hypothermia, or both, on messenger RNA gene expression in the human diaphragm. We hypothesized that the expression of stress response, redox regulation, and proteolysis genes would be predominantly increased during the course of CTS, whereas energy metabolism, cell cycle, and contractile function would be predominantly decreased.

MATERIALS AND METHODS

Subjects

As a sample of convenience, 6 male patients 50 years old or older undergoing aortic repair were recruited for this prospective, observational, and repeated-measures design study. One subject (patient 2) was excluded as a result of technical failure with the analysis; thus there were only 5 subjects' specimens used in the final analysis. The institutional review broad at University of Florida approved the protocol, and participants gave their written consent. The exclusion criteria consisted of New York Heart Association functional class III or IV cardiac disease; history of stroke, cerebrovascular disease, spinal cord injury, or progressive neuromuscular disease; CTS within the previous 12 weeks; a history of pneumonectomy or lung surgery; skeletal pathology, such as scoliosis; forced expiratory volume in 1 second less than 60% of the age-predicted value; and malignancy.

Surgical Procedure

All patients underwent a median sternotomy and CPB. Patients undergoing arch aortic surgery were selected because of the longer surgical time course, and all operations were performed by the same surgeon (T.M.B.). Hypothermic CPB (temperatures of 18°C–24°C) with antegrade and retrograde blood cardioplegia was used in all cases, with brief periods of hypothermic circulatory arrest during the proximal arch anastomosis. A 1-g bolus of methylprednisolone sodium succinate (Solu-medrol; Pharmacia and Upjohn, Kalamazoo, Mich) was in the prime solution on initiation of CPB. During CPB, mean arterial pressure of 50 to 80 mm Hg and blood flows of 2.4 to 2.8 L/(min · m^2) were maintained. The hematocrit was maintained above 20% during CPB. The use of vasoactive drugs was at the discretion of the anesthesiologist managing the case. Patients were actively rewarmed to 36.5°C before weaning from CPB. After surgery, all patients were transferred to the cardiothoracic intensive care unit for recovery.

Anesthetic Management

A preoperative dose of vancomycin (1–4 mg) was given intravenously. A standard anesthesia regimen was used in all patients. Subjects were intubated and administered general anesthesia by the anesthesiologist. Controlled MV was maintained at 5 cycles/min with a tidal volume of 5 to 7 mL/kg. Anesthetic induction consisted of fentanyl, propofol, midazolam (Versed; F. Hoffmann-La Roche AG, Basel, Switzerland), vancomycin, and vecuronium bromide. Intraoperative paralysis was sustained with vecuronium bromide (0.6–0.8 mg/kg) or pancuronium bromide (0.1–0.12 mg/kg).

Diaphragm Biopsies

Two full-thickness biopsy specimens (approximately 6 mm in diameter) were taken from mirror-image locations of the anterolateral aspect of the right and left hemidiaphragms near the costal margins. The first biopsy specimen was obtained immediately after exposure of the diaphragm; the second biopsy specimen was obtained as late during surgery as possible. Tissue samples were blotted to remove visible blood. Each specimen was stabilized by using RNAlater solution (Ambion Inc, Applied Biosystems by Life Technologies Corporation, Carlsbad, Calif) and then transferred to liquid nitrogen and stored at –80°C until analysis.

RNA Isolation

The online data supplement gives details of the RNA isolation.

Complementary RNA Synthesis and Microarray Hybridization

Complementary RNA was synthesized according to the 2-step amplification protocol outlined by the manufacturer (Affymetrix UK Ltd, High Wycombe, UK), with 0.4 μg of total RNA as starting material. Second, complementary RNA was transcribed in vitro with the incorporation of biotinylated nucleotides with an ENZO Bio Array High Yield RNA Transcript Labeling Kit (T7; Enzo Life Sciences Inc, Farmingdale, NY), and the biotin-labeled product was hybridized onto an Affymetrix Hu U133 plus 2.0 GeneChip, which contains 54,675 probe sets representing more than 38,500 well-substantiated human genes. Staining and washing followed the protocol (EukGEWSv4; Affymetrix) with a fluidics station (Affymetrix).

Statistical Analysis of Affymetrix Microarray Gene Expression

Data acquisition (scanning). The arrays were scanned with a scanner (Affymetrix), and the fluorescence intensity was calculated with Affymetrix Gene Chip Operating Software. Chip-to-chip normalization was accomplished with dChip (Wong laboratory, Department of Biostatistics, Harvard School of Public Health, Cambridge, Mass) normalization protocols. An expression matrix was modeled with the perfect match–only model algorithms of dChip. The details of this model are described elsewhere.[12]

Gene Chip Operating Software was used to identify probe sets in which the hybridization signal intensity was at or below background levels. Signals in these probe sets were considered to be absent. Probe sets in which the signal intensity was absent on all arrays under study were excluded in the following 2-step high-level statistical analysis.

Unsupervised analysis of gene expression patterns. Unsupervised analysis was performed with probe sets in which the hybridization signal intensities varied the most across the data set. Probe sets with a coefficient of variation greater than 0.5 were identified and subjected to hierarchic cluster analysis with dChip clustering algorithms.[12]

Supervised analysis of gene expression patterns. The dChip expression matrix was filtered to remove probe sets that were never detected above background on any array in the analysis. Of the 10 arrays investigated, the expression of 2558 probe sets was not above background on any array from the 54,675 probe sets present in the Affymetrix Hu U133 plus 2.0 GeneChip. Of the remaining 52,117 probe sets detected above background on at least 1 array, 3318 probe sets exceeded the coefficient of variation filter of greater than 0.5 and were subsequently subjected to hierarchic cluster analysis (Figure 1, and see E-Materials and Methods for details). This expression matrix was imported to BRB Array Tools (v3.4 Beta 2; http//linus.nci.nih.gov/BRB-ArrayTools.html) for supervised analysis. BRB Array Tools was used to identified genes that were differentially expressed between early-surgery and late-surgery samples (paired by patients) at the $P <$ .005 level of significance (according to a modified Student t test). This supervised analysis identified 1080 probe sets differentially expressed (early vs late samples) at $P < .005$.

Once probe sets had been identified that were differentially expressed between early-surgery and late-surgery samples, NetAffx query (http://www.affymetrix.com/analysis/index.affx) was undertaken for retrieving Gene Ontology annotations of the significant probe sets. In addition, tabular gene expression data were published online in the Gene Expression Omnibus (http://www.ncbi.nlm.nih.gov/geo/), submission GSE19533.

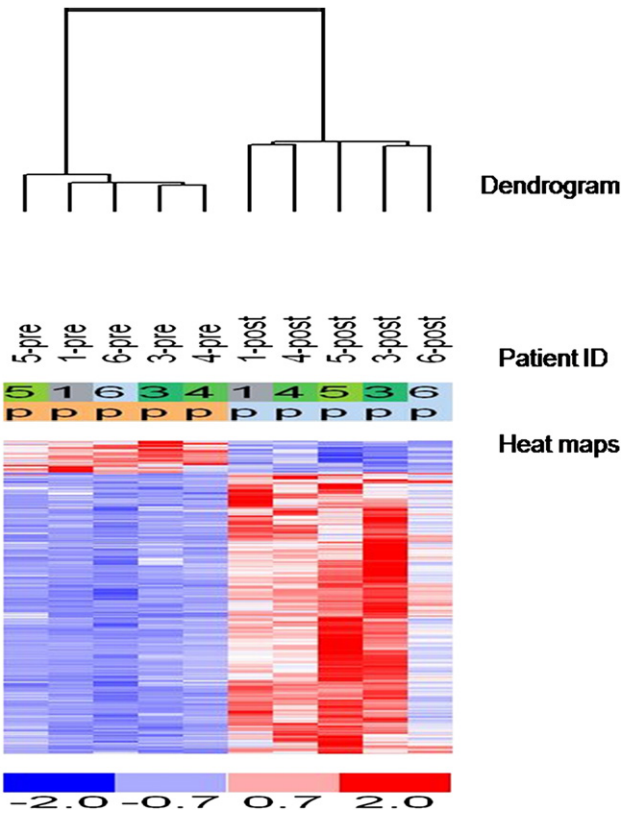

FIGURE 1. This figure shows the hierarchic cluster pattern of the hybridization signal intensities of 3318 probe sets that display a coefficient of variation greater than 0.5. In the heat map, the intensity of the color indicates relative expression for each individual gene. The dendrogram of the clustering *(top)* is used to identify similarities in expression patterns among the arrays.

Functional classification. Genes identified as significantly different by microarray were grouped according to 2 public databases: Gene Ontology (http://www.ncbi.nih.gov/entrez/query.fcgi?db=OMIM) and NetAffx (http://www.affymetix.com/analysis/netaffx/goanalysis_netaffx4.affx).

Pathway analysis. For the 779 unique known identified genes, the Pathway-Express, part of a package of microarray tools (http://vortex.cs.wayne.edu/projects.htm) was used to provide searchable pathways that related to the significant gene products in our study. The Pathway-Express database currently contains signaling pathways from Kyoto Encyclopedia of Genes and Genomes (http://www.genome.jp/kegg/). The Pathway-Express performed a classic enrichment analysis that was based on a hypergeometric distribution to identify those pathways that contained a proportion of differentially expressed genes that was significantly different from that expressed just by chance.[13]

Microarray Validation by Quantitative Real-Time Reverse Transcriptase Polymerase Chain Reaction

After the microarray analysis, selected genes were chosen for validation by quantitative real-time reverse transcriptase polymerase chain reaction. Gene selection was based on the magnitude of change in expression and the relevance to skeletal muscle protein regulation. The following 5 genes were selected: cathepsin L1 *(CTSL1),* F-box protein 32 *(FBXO32),* myocyte enhancer factor 2C *(MEF2C),* superoxide dismutase 2 *(SOD2),* mitochondrial and tripartite motif-containing 63 *(TRIM63).* The online supplement gives details of the quantitative real-time reverse transcriptase polymerase chain reaction procedure. Fold change values obtained from microarray and reverse transcriptase polymerase chain reaction analysis were compared with Pearson correlation.

RESULTS

Patient Collective and Clinical Data

The patients' demographic and clinical characteristics are given in Table 1. The average MV duration before the first biopsy sample was taken was 124 ± 19 minutes; the average MV duration before the second biopsy sample was taken was 415 ± 112 minutes. The elapsed time between muscle biopsies was 4.9 ± 1.8 hours. CPB time ranged from 159 to 266 minutes, with a mean ± SD of 218 ± 51 minutes. One of the 5 subjects did not require hypothermic circulatory arrest because the aortic arch was replaced under selective antegrade perfusion, although the body was cooled to 18°C for cerebral protection. All subjects tolerated surgery and both biopsies without event, and no study-related postoperative complications were noted.

Microarray Data Analysis and Biostatistics

Microarray data analysis identified 1080 probe sets that were differentially expressed (early vs late samples, $P <$ .005). Among these 1080 probe sets, 779 unique known genes were identified. Most of the transcripts (616/779, 79%) were upregulated. The pathway analysis revealed that janus kinase/signal transducers and activators of

TABLE 1. Clinical baseline characteristics of 5 patients undergoing cardiothoracic surgery

Case	Age (y)	Height (cm)	Weight (kg)	Comorbidities	Type of surgery	CPB time (min)	HCA time (min)	CP time (min)
1	56	183	155	Tracheostomy, morbid obesity, obstructive lung defect, decreased oxygen diffusion capacity, obstructive sleep apnea	AVR, ascending and proximal arch aorta	243	15	202
3	76	174	87	Aortic insufficiency, CAD, chronic renal insufficiency, hypertension, prostate cancer with radiation, bladder disorder with chronic UTIs, urethral strictures	AVR, ascending and proximal arch aorta	159	10	135
4	71	182	100	DeBakey type 2 aortic dissection, hypertension, abdominal artery aneurysm, COPD	Ascending and proximal arch aorta	166	24	42
5	54	183	110	Severe aortic insufficiency, dilated cardiomyopathy (EF 40%), CAD	Ascending and proximal arch aorta	266	5	204
6	78	180	100	CAD, hypertension, diabetes mellitus	Aortic root valve-sparing procedure	255	NA	130
Mean	67	180	110			218	13.5	142
SD	11	4	26			51	8	66

CPB, Cardiopulmonary bypass; *HCA,* hypothermic circulatory arrest; *CP,* crossclamp; *AVR,* aortic valve replacement; *CAD,* coronary artery disease; *UTI,* urinary tract infection; *COPD,* chronic obstructive pulmonary disease; *EF,* ejection fraction; *NA,* not applicable.

transcription (JAK-STAT) and p53 signaling pathways were significantly overexpressed ($P < .0001$).

A NetAffx query was performed to retrieve Gene Ontology classifications of the differently expressed genes, which were grouped into 11 functional categories (Table E1). Because we expected a large number of genes to be differentially expressed, a priori we elected to narrow our discussion to selected physiologically relevant categories, including the stress response and redox regulation (Tables 2 and E2), protein turnover and energy metabolism (Tables 3 and E3), and muscle-specific and neuromuscular regulatory genes (Table 4). The remaining functional categories and the list of expressed sequence tags are summarized in the online data supplement (Tables E2–E11).

In the stress response and redox regulation category, we identified 86 differentially expressed transcripts linked to regulation of inflammation and chemotaxis, the JAK-STAT cascade, and redox regulation. Two inflammatory and chemotaxis response genes, IL6 and IL8, showed the highest fold changes at 15.6-fold and 22.7-fold, respectively. Genes responsible for redox regulation included peroxiredoxin 6 (*PRDX6,* 1.9-fold), superoxide dismutase in mitochondria (*SOD2,* 2.9-fold), thioredoxin (*TXN,* 1.9-fold), selenoprotein S (*SELE,* 1.5-fold), and a number of the metallothioneins (Table E2). Changes in redox regulation were accompanied by a large upregulation of cell cycle genes, including a significant overexpression of the p53 pathway.

In the protein turnover and energy metabolism category, differentially-expressed genes were linked to lysosomal activity, protein folding, protein synthesis, and the ubiquitin-proteasome–dependent pathway. We found that messenger RNAs for the ubiquitin-proteasome–dependent pathway were upregulated, including several ubiquitin-conjugating enzymes (1.5- to 1.8-fold), ubiquitin-specific peptidases (1.8- to 2.2-fold), and 1 muscle-specific ubiquitin protein ligase enzyme (the E3 ligase MuRF-1, gene *TRIM63,* 2.6-fold). Interestingly, another well-known gene associated with muscle atrophy, F-box protein 32 *(FBXO32),* also known as MAF-box, was significantly downregulated (Table 3). We also identified differentially expressed transcripts related to carbohydrate metabolism, glucose transport, and lipid metabolism (Table E3).

In the muscle-specific and neuromuscular regulatory category, differential expressions occurred in genes linked to sarcomere structure and function and to neuromuscular synaptic transmission (Table 4).

Quantitative Real-Time Reverse Transcriptase Polymerase Chain Reaction

The results from quantitative real-time reverse transcriptase polymerase chain reaction showed excellent agreement with those of the microarray. A significant correlation was observed between gene array changes and quantitative real-time reverse transcriptase polymerase chain reaction ($r = 0.95$, $P < .0001$).

DISCUSSION

Genome-wide gene expression profiling has enabled scientists to investigate complex biologic processes regulated at the transcriptional level. In this study, we examined the gene expression profile of human diaphragm muscles from 5 clinically scheduled patients who underwent CTS. The combined effects of CPB, hypothermia, anesthesia, fasting, and controlled MV resulted in 779 unique transcripts that were differentially expressed ($P < 0.005$) between early and late CTS periods. Diaphragm gene

TABLE 2. List of key genes related to stress response and redox regulation that were significantly different after surgery

Probe set	Symbol	Fold*	*P* value	Description	Function
Regulation of inflammation and chemotaxis					
216598_s_at	*CCL2*	8.2	1.2E–6	Chemokine (C-C motif) ligand 2	Inflammatory response
202859_x_at	*IL8*	22.7	1.1E–3	Interleukin 8	Mediates neutrophil chemotaxis and migration
218995_s_at	*EDN1*	1.8	3.1E–3	Endothelin 1	Neutrophil chemotaxis
201925_s_at	*CD55*	2.0	3.0E–3	CD55 molecule, decay-accelerating factor for complement (Cromer blood group)	Immune response
204908_s_at	*BCL3*	3.9	9.9E–6	B-cell chronic lymphocytic leukemia/ lymphoma 3	T-helper 1–type immune response
204748_at	*PTGS2*	5.2	4.0E–4	Prostaglandin-endoperoxide synthase 2 (prostaglandin G/H synthase and cyclooxygenase)	Response to cytokine stimulus
221477_s_at	*MGC5618*	1.6	4.3E–3	Hypothetical protein MGC5618	Response to oxidative stress
JAK-STAT signaling					
209682_at	*CBLB*	1.8	1.9E–3	Cas-Br-M (murine) ecotropic retroviral transforming sequence b	Regulator of JAK-STAT signaling
205207_at	*IL6*	15.6	3.5E–5	Interleukin 6 (interferon β2)	Mediates leukocytosis, thrombosis, and lymphocyte activation
1552611_a_at	*JAK1*	1.5	4.3E–3	Janus kinase 1 (a protein tyrosine kinase)	Couples cytokine ligand binding to STAT signaling
210001_s_at	*SOCS1*	4.7	1.0E–6	Suppressor of cytokine signaling 1	JAK-STAT cascade
203372_s_at	*SOCS2*	3.1	2.7E–5	Suppressor of cytokine signaling 2	JAK-STAT cascade
227697_at	*SOCS3*	9.4	1.1E–5	Suppressor of cytokine signaling 3	JAK-STAT cascade
208992_s_at	*STAT3*	1.6	2.0E–3	Signal transducer and activator of transcription 3 (acute-phase response factor)	JAK-STAT cascade
Cell cycle regulation (p53 signaling)					
203725_at	*GADD45A*	3.0	4.5E–4	Growth arrest and DNA damage–inducible, α	Cell cycle regulator
209305_s_at	*GADD45B*	10.2	5.3E–6	Growth arrest and DNA damage–inducible, β	Cell cycle regulator
204121_at	*GADD45G*	4.3	1.8E–6	Growth arrest and DNA damage–inducible, γ	Cell cycle regulator
Redox regulation					
242751_at	*PRDX6*	1.9	6.3E–4	Peroxiredoxin 6	Cell redox homeostasis
215223_s_at	*SOD2*	2.9	1.1E–5	Superoxide dismutase 2, mitochondrial	Cell redox homeostasis
208864_s_at	*TXN*	1.9	2.9E–3	Thioredoxin	Cell redox homeostasis
223209_s_at	*SELS*	1.5	4.0E–3	Selenoprotein S	Cell redox homeostasis: regulated by glucose deprivation and endoplasmic reticulum stress
217546_at	*MT1M*	11.4	6.0E–7	Metallothionein 1M	Metallothioneins may inhibit reactive oxygen species and protect against DNA damage

JAK-STAT, Janus kinase/signal transducers and activators of transcription. **Fold* denotes fold change between presurgical and postsurgical conditions.

expression underwent a distinct pattern of changes in specific pathways that included upregulation of inflammation, redox regulation, and protein turnover genes, as well as downregulation of some of energy metabolism, cell cycle, and neuromuscular function genes.

Inflammatory Mediators

We found a robust and diverse expression of inflammatory and stress-responsive genes in the diaphragm during the course of CTS. The pathway analysis revealed strongly significant overexpression of JAK-STAT signaling ($P < .0001$). JAK-STAT signaling regulates cellular responses to cytokines and growth factors through binding to IL-6, with downstream phosphorylation of 1 or more signal transducer and activator of transcription molecules. The proinflammatory cytokine IL-6 was highly upregulated (15.6-fold), and it may be upregulated in response to thermal stress as well as CPB. Significant increases of inflammatory gene expressions, including those for IL-6 and IL-8, have also been reported in human intercostal muscles after an average 74 minutes of CPB.[11] Of the 32 upregulated genes reported in the intercostals, 14 were similarly elevated in the diaphragms of our patients, and a large number of these served stress-responsive functions. It has been hypothesized that both systematic inflammatory responses and intrinsic oxidative stress result in impaired diaphragm neuromuscular transmission during CPB.[8] We have previously shown in patients undergoing complex cardiac surgery that those patients with the highest circulating levels of IL-6 and IL-10 had greater morbidity postoperatively, including prolonged ventilation and longer intensive care unit stay.[14]

TABLE 3. Expression of protein turnover and energy metabolism key genes that were significantly different in the diaphragm after surgery

Probe set	Symbol	Fold*	*P* value	Description	Function
Thermosensitive regulatory genes					
200881_s_at	*DNAJA1*	1.9	2.9E–3	DnaJ (heat shock protein 40) homolog, subfamily A, member 1	Chaperone-mediated protein folding requiring cofactor
201041_s_at	*DUSP1*	3.7	8.8E–4	Dual specificity phosphatase 1	Thermal sensitive mitogen-activated protein kinase inhibitor, may inhibit cellular proliferation
Proteolysis-related genes					
225647_s_at	*CTSC*	2.7	2.1E–3	Cathepsin C	Lysosome
202087_s_at	*CTSL1*	2.0	2.8E–3	Cathepsin L1	Lysosome
202723_s_at	*FOXO1*	1.9	2.0E–3	Forkhead box O1	Transcriptional regulator of ubiquitin ligases
204131_s_at	*FOXO3*	1.7	2.0E–3	Forkhead box O3	Transcription factor; regulates ubiquitin ligases, neutral factor κB signaling, and p53 activity
231990_at	*USP15*	2.2	1.5E–4	Ubiquitin specific peptidase 15	Ubiquitin thiolesterase activity
241762_at	*FBXO32*	–3.5	5.6E–5	F-box protein 32	Ubiquitin-dependent protein catabolic process
236972_at	*TRIM63*	2.6	4.1E–5	Tripartite motif-containing 63	Ubiquitin-dependent protein catabolic process
243046_at	*UBE2D3*	1.8	7.1E–4	Ubiquitin-conjugating enzyme E2D 3 (UBC4/5 homolog, yeast)	Ubiquitin–protein ligase activity
202779_s_at	*UBE2S*	1.6	1.1E–3	Ubiquitin-conjugating enzyme E2S	Ubiquitin–protein ligase activity
Protein translation–related genes					
225954_s_at	*MIDN*	3.4	1.3E–6	Midnolin	Protein modification
223481_s_at	*MRPL47*	–1.8	8.9E–4	Mitochondrial ribosomal protein L47	Protein synthesis
201574_at	*ETF1*	3.4	3.0E–3	Eukaryotic translation termination factor 1	Protein synthesis
224873_s_at	*MRPS25*	–1.4	5.0E–3	Mitochondrial ribosomal protein S25	Protein synthesis
Apoptosis-related genes					
201101_s_at	*BCLAF1*	3.4	3.6E–3	*BCL2*-associated transcription factor 1	Interact with B-cell lymphoma 2–related proteins
205681_at	*BCL2A1*	3.4	3.8E–3	*BCL2*-related protein A1	Interact with B-cell lymphoma 2–associated X protein isoform sigma
209189_at	*FOS*	3.4	1.9E–3	*v-fos* FBJ murine osteosarcoma viral oncogene homolog	Apoptotic regulation
201473_at	*JUNB*	3.4	2.6E–5	B-*jun* proto-oncogene	Response to cytokine stimulus; proapoptotic transcription factor acting with *FOS*
Energy metabolism genes					
205960_at	*PDK4*	3.4	3.5E–3	Pyruvate dehydrogenase kinase, isozyme 4	Glucose metabolism
235374_at	*MDH1*	–2.2	2.3E–3	Malate dehydrogenase 1, nicotinamide adenine dinucleotide (soluble)	Glycolysis
208383_s_at	*PCK1*	–2.3	1.3E–3	Phosphoenolpyruvate carboxykinase 1 (soluble)	Regulation of gluconeogenesis

**Fold* denotes fold change between presurgical and postsurgical conditions.

Redox Regulation

Oxidative stress has been implicated as a major contributor to ventilator-induced diaphragm dysfunction in animals, and significant oxidative stress occurs with as little as 3 to 6 hours of controlled MV.[15] CPB also elicits acute oxidative stress in cardiac and skeletal myofibers, which may contribute to post-CPB myocardial dysfunction.[16] In this study, we found that several genes responsible for attenuating oxidative stress were upregulated, including the endogenous antioxidant genes *SOD2, PRDX6,* and *TXN* (Table 2). Moreover, robust upregulation of metallothionein genes can occur in response to fasting, inactivity, or rewarming after cold exposure,[2,17,18] and their transcription may protect skeletal muscle from lipid peroxidation and contractile dysfunction.[4] In conjunction with upregulated stress response signaling and an altered redox state, gene expression favored cell cycle arrest. In particular, the pathway analysis revealed overexpression of the p53 signaling pathway, which transcriptionally inhibits cell cycle progression in the presence of DNA damage and can facilitate cell apoptosis. Upregulation of cell cycle arrest gene expression has been reported separately during instances of MV, CPB, hypothermia, and fasting.[4,11,17,18]

Protein Turnover

MV-induced diaphragm atrophy has been linked to significant activity of the calcium-activated, proteosomal, and neutral factor κB pathways.[15] The ubiquitin-proteasome pathway is thought to control the majority of myofibrillar protein breakdown during muscle wasting,[19] and the E3 ubiquitin ligases MAF-box and MuRF-1 have been implicated in animal models of inactivity[15] and inflammation-mediated disuse atrophy.[20] We found that genes for MuRf-1 and several atrophy-related

TABLE 4. List of muscle specific and neuromuscular regulatory genes that were significantly different in the diaphragm after surgery

Probe set	Symbol	Fold*	*P* value	Description	Function
Sarcomere structure and function					
215795_at	*MYH7B*	–2.4	4.3E–3	Myosin, heavy chain 7B, cardiac muscle, β	Actin binding
222976_s_at	*TPM3*	1.6	3.2E–3	Tropomyosin 3	Actin binding
1567107_s_at	*TPM4*	2.1	1.0E–3	Tropomyosin 4	Actin binding
1569512_at	*SVIL*	1.9	7.5E–4	Supervillin	Actin filament binding
242795_at	*MYOT*	–2.8	2.5E–3	Myotilin	Actin filament stabilization during muscle contraction
211926_s_at	*MYH9*	1.7	4.4E–3	Myosin, heavy chain 9, nonmuscle	Actin cytoskeletal reorganization
207424_at	*MYF5*	–1.6	1.9E–3	Myogenic factor 5	Myogeneic differentiation
206657_s_at	*MYOD1*	2.0	4.0E–3	Myogenic differentiation 1	Myogeneic differentiation
236395_at	*MEF2C*	–3.5	1.4E–4	Myocyte enhancer factor 2C	Terminal differentiation; thick filament organization
206201_s_at	*MEOX2*	–3.5	6.1E–4	Mesenchyme homeobox 2	Muscle differentiation
Synaptic transmission					
200815_s_at	*PAFAH1B1*	1.4	4.8E–3	Platelet-activating factor acetylhydrolase, isoform Ib, α subunit 45 kDa	Neuromuscular process controlling balance
204224_s_at	*GCH1*	4.6	6.3E–5	Guanosine triphosphate cyclohydrolase 1 (dopa-responsive dystonia)	Neuromuscular process controlling posture
206115_at	*EGR3*	4.1	4.9E–3	Early growth response 3	Neuromuscular synaptic transmission
206552_s_at	*TAC1*	5.0	2.0E–5	Tachykinin, precursor 1	Positive regulation of synaptic transmission, γ-aminobutyric acid–ergic
201693_s_at	*EGR1*	6.7	2.3E–3	Early growth response 1	Regulation of long-term neuronal synaptic plasticity
210090_at	*ARC*	10.7	1.2E–5	Activity-regulated cytoskeleton-associated protein	Regulation of neuronal synaptic plasticity
201170_s_at	*BHLHB2*	2.7	1.3E–5	Basic helix-loop-helix domain containing, class B2	Regulation of neuronal synaptic plasticity
205249_at	*EGR2*	6.1	3.4E–3	Early growth response 2 (Krox-20 homolog, *Drosophila*)	Regulation of neuronal synaptic plasticity
215483_at	*AKAP9*	–1.5	2.7E–3	Kinase (PRKA) anchor protein (yotiao) 9	Synaptic transmission
241652_x_at	*LIN7A*	2.1	2.0E–3	Lin-7 homolog A (*Caenorhabditis elegans)*	Synaptic transmission

**Fold* denotes fold change between presurgical and postsurgical conditions.

ETJBS

ubiquitin-conjugating enzymes (E2) were upregulated, whereas the gene expression of MAF-box was actually downregulated (Table 3). The *FOX1* and *FOXO3* transcription factor genes, important upstream regulators of MAFbx and MuRf-1, were upregulated. Increased expressions of ubiquitin-proteasome–dependent pathway genes and the gene for cathepsin L observed in our patients have also been reported in rodents subjected to prolonged MV.[21] In addition to early activity of genes related to the ubiquitin-proteasome–dependent pathway noted in our patients, the apoptosis-regulating *BCL2* gene was overexpressed. We did not, however, find significant differences in downstream proapoptotic caspase genes. These results suggest that acute mediators of atrophy and apoptosis were rapidly activated during CTS, and we hypothesize that longer durations of MV are required for significant effects on downstream proteolytic and apoptotic gene expressions.

Energy Metabolism

Observed changes in energy metabolism gene expression suggest reduced energy use by the diaphragm during CTS (Table 3). Upregulation of *PDK4,* a negative moderator of mitochondrial pyruvate dehydrogenase, results in decreased mitochondrial use of glucose. Interestingly, MuRF1 directly targets *PDK4,* and transcriptional facilitation of *PDK4* could reflect MuRF1 transcriptional regulation of protein synthesis, proteolysis, and preservation of the amino acid pool.[22] Expression of *MDH1* was downregulated during CTS and corresponded with other MV inactivity models.[4] Decreased *MDH1* expression suggests suppression of the malate shuttle and could occur as a consequence either of reduced energetic requirements or of a limited ability for the mitochondria to process reduced nicotinamide adenine dinucleotide.

Sarcomere Structure

Short periods of diaphragm inactivity during surgery were associated with upregulation of myofilament stabilization genes (Table 4). These structural and costameric molecules may collectively act as stabilizers and force-couplers between the sarcomere and plasma membrane, and they may initiate cell cascades in response to altered mechanical

loads.[23] Cold stress can also modify expression of structural genes as a response to maintain phospholipid membrane fluidity.[18] Still, limited research is available regarding the transcriptional remodeling of the supportive proteins during the course of CTS.

Neuromuscular Function

Eleven of the upregulated genes promoted neural plasticity and synaptic transmission (Table 4). Anesthesia was induced after a short infusion of neuromuscular blockade at the onset of surgery; however, blockade was not continued throughout the procedure. Thus baseline synaptic transmission gene expression may have been relatively depressed relative to late surgery. Although thoracic cooling can decrease phrenic nerve conduction and increase evoked diaphragm latency, late surgical rewarming may have accounted for the upregulation in synaptic gene expression observed in our patients.[9]

In addition to differential synaptic gene expression, myogenic-specific genes were upregulated, including *MYOD, MEOX2,* and *MEF2C.* Coexpression of myogenic-specific genes and cell cycle inhibitors has been seen to increase acutely in other disuse atrophy models.[24]

Limitations

Microarrays allow simultaneous analysis of the expressions of thousands of genes; however, the microarray results for any given gene are often noisy or ambiguous. Microarrays are potentially influenced by many external factors, including array production, RNA extraction methods, the probes used for labeling, hybridization conditions, and image analysis.[25] Despite the small sample size in this study, we nevertheless found substantial changes in diaphragm gene expression and verified the microarray results by an independent method. Conventionally, quantitative real-time reverse transcriptase polymerase chain reaction is the method of choice for validation, because it is a sensitive, high-throughput procedure that requires a minimal amount of test material.[25] The results from quantitative real-time reverse transcriptase polymerase chain reaction showed excellent agreement with the microarray analysis with respect to both direction and magnitude of change ($r = 0.95$, $P < .0001$).

The CTS model used in this study offers both benefits and challenges. Understandably, we could not include a control group; however, the repeated measures design enabled subjects to serve as their own controls. The model was not a pure MV inactivity paradigm; in addition to controlled MV, it included general anesthesia, CPB, surgical repair, hypothermia, and short-term fasting. The stressors of surgery and quiescence, however, negatively impacted diaphragm gene expression. Recent work has shown that neuromuscular blockade and CPB impair diaphragm contractility and neuromuscular transmission independently of the effects of MV alone.[8]

Although our patients were classified as at low preoperative risk for ventilator-induced diaphragm dysfunction, the multifactorial stressors of surgery significantly increased the expression of genes implicated in inflammation, proteolysis, and cell cycle arrest. Diaphragm biopsy specimens from patients with chronic obstructive pulmonary disease illustrate that oxidative stress and proteolysis are significantly elevated at baseline.[26] Additional CTS stressors could potentially place patients with preexisting respiratory muscle dysfunction at greater risk for postoperative weaning failure and ventilator-induced diaphragm dysfunction.[27]

CONCLUSIONS

This study has demonstrated that CTS results in rapid changes in human diaphragm gene expression. We identified 779 transcripts that were differentially expressed ($P < .005$) between early and late surgical samples. The major findings are as follows: (1) Inflammatory and stress-related genes demonstrated the largest changes, including an overexpression of JAK-STAT and p53 signaling. (2) An increased expression of antioxidant genes occurred, which may be a protective adaptation in response to CTS. (3) Atrophy-related gene expression occurred rapidly in the diaphragm. (4) Gene expression for energy metabolism indicated a low bioenergetic state, with ongoing attempts to conserve the glucose and amino acid pool. We speculate that some of the messenger RNA changes seen in this study could represent an early response to diaphragm muscle inactivity and surgical stressors in a subject cohort with a low risk of ventilator-induced diaphragm dysfunction. The rapid changes that we observed in gene expression may be relevant to understanding diaphragm plasticity during CTS. Continued investigation is warranted with patients who may be at increased risk for development of postsurgical respiratory muscle complications, such as those with low bioenergetic reserves, preexisting inflammatory states, or impaired regenerative capacity.

We thank M. Cecilia Lopez, BS, as well as Sharon Norton, MS, for technical support of the study.

References

1. Trouillet JL, Combes A, Vaissier E, Luyt CE, Ouattara A, Pavie A, et al. Prolonged mechanical ventilation after cardiac surgery: outcome and predictors. *J Thorac Cardiovasc Surg*. 2009;138:948-53.
2. Powers SK, Kavazis AN, Levine S. Prolonged mechanical ventilation alters diaphragmatic structure and function. *Crit Care Med*. 2009;37(10 Suppl): S347-53.
3. Powers SK, Shanely RA, Coombes JS, Koesterer TJ, McKenzie M, Van Gammeren D, et al. Mechanical ventilation results in progressive contractile dysfunction in the diaphragm. *J Appl Physiol*. 2002;92:1851-8.
4. DeRuisseau KC, Shanely RA, Akunuri N, Hamilton MT, Van Gammeren D, Zergeroglu AM, et al. Diaphragm unloading via controlled mechanical ventilation alters the gene expression profile. *Am J Respir Crit Care Med*. 2005;172: 1267-75.

5. Sassoon CS, Zhu E, Caiozzo VJ. Assist-control mechanical ventilation attenuates ventilator-induced diaphragmatic dysfunction. *Am J Respir Crit Care Med*. 2004;170:626-32.
6. Gayan-Ramirez G, Testelmans D, Maes K, Rácz GZ, Cadot P, Zádor E, et al. Intermittent spontaneous breathing protects the rat diaphragm from mechanical ventilation effects. *Crit Care Med*. 2005;33:2804-9.
7. Levine S, Nguyen T, Taylor N, Friscia ME, Budak MT, Rothenberg P, et al. Rapid disuse atrophy of diaphragm fibers in mechanically ventilated humans. *N Engl J Med*. 2008;358:1327-35.
8. Ermilov LG, Pulido JN, Atchison FW, Zhan WZ, Ereth MH, Sieck GC, et al. Impairment of diaphragm muscle force and neuromuscular transmission after normothermic cardiopulmonary bypass: effect of low-dose inhaled CO. *Am J Physiol Regul Integr Comp Physiol*. 2010;298:R784-9.
9. Mills GH, Khan ZP, Moxham J, Desai J, Forsyth A, Ponte J. Effects of temperature on phrenic nerve and diaphragmatic function during cardiac surgery. *Br J Anaesth*. 1997;79:726-32.
10. Testelmans D, Maes K, Wouters P, Gosselin N, Deruisseau K, Powers S, et al. Rocuronium exacerbates mechanical ventilation-induced diaphragm dysfunction in rats. *Crit Care Med*. 2006;34:3018-23.
11. Ruel M, Bianchi C, Khan TA, Xu S, Liddicoat JR, Voisine P, et al. Gene expression profile after cardiopulmonary bypass and cardioplegic arrest. *J Thorac Cardiovasc Surg*. 2003;126:1521-30.
12. Li C, Hung Wong W. Model-based analysis of oligonucleotide arrays: model validation, design issues and standard error application. *Genome Biol*. 2001;2. RESEARCH0032.
13. Khatri P, Voichita C, Kattan K, Ansari N, Khatri A, Georgescu C, et al. OntoTools: new additions and improvements in 2006. *Nucleic Acids Res*. 2007 Jul; 35(Web Server issue):W206-11.
14. Kim T, Arnaoutakis GJ, Bihorac A, Martin TD, Hess PJ Jr, Klodell CT, et al. Early blood biomarkers predict organ injury and resource utilization following complex cardiac surgery. J Surg Res. Epub 2009 Oct 6.
15. Powers SK, Kavazis AN, McClung JM. Oxidative stress and disuse muscle atrophy. *J Appl Physiol*. 2007;102:2389-97.
16. Ramlawi B, Otu H, Mieno S, Boodhwani M, Sodha NR, Clements RT, et al. Oxidative stress and atrial fibrillation after cardiac surgery: a case-control study. *Ann Thorac Surg*. 2007;84:1166-73.
17. Lecker SH, Jagoe RT, Gilbert A, Gomes M, Baracos V, Bailey J, et al. Multiple types of skeletal muscle atrophy involve a common program of changes in gene expression. *FASEB J*. 2004;18:39-51.
18. Sonna LA, Fujita J, Gaffin SL, Lilly CM. Invited review: effects of heat and cold stress on mammalian gene expression. *J Appl Physiol*. 2002;92:1725-42.
19. Attaix D, Ventadour S, Codran A, Béchet D, Taillandier D, Combaret L. The ubiquitin-proteasome system and skeletal muscle wasting. *Essays Biochem*. 2005;41:173-86.
20. Bodine SC, Latres E, Baumhueter S, Lai VK, Nunez L, Clarke BA, et al. Identification of ubiquitin ligases required for skeletal muscle atrophy. *Science*. 2001; 294:1704-8.
21. Deruisseau KC, Kavazis AN, Powers SK. Selective downregulation of ubiquitin conjugation cascade mRNA occurs in the senescent rat soleus muscle. *Exp Gerontol*. 2005;40:526-31.
22. Koyama S, Hata S, Witt CC, Ono Y, Lerche S, Ojima K, et al. Muscle RING-finger protein-1 (MuRF1) as a connector of muscle energy metabolism and protein synthesis. *J Mol Biol*. 2008;376:1224-36.
23. Frank D, Kuhn C, Katus HA, Frey N. The sarcomeric Z-disc: a nodal point in signalling and disease. *J Mol Med*. 2006;84:446-68.
24. Stevenson EJ, Giresi PG, Koncarevic A, Kandarian SC. Global analysis of gene expression patterns during disuse atrophy in rat skeletal muscle. *J Physiol*. 2003; 551(Pt 1):33-48.
25. Chuaqui RF, Bonner RF, Best CJ, Gillespie JW, Flaig MJ, Hewitt SM, et al. Post-analysis follow-up and validation of microarray experiments. *Nat Genet*. 2002; 32(Suppl):509-14.
26. Marin-Corral J, Minguella J, Ramirez-Sarmiento AL, Hussain SN, Gea J, Barreiro E. Oxidised proteins and superoxide anion production in the diaphragm of severe COPD patients. *Eur Respir J*. 2009;33:1309-19.
27. Cislaghi F, Condemi AM, Corona A. Predictors of prolonged mechanical ventilation in a cohort of 5123 cardiac surgical patients. *Eur J Anaesthesiol*. 2009;26:396-403.

E-MATERIALS AND METHODS

Isolation of Total RNA

Total RNA was isolated with the RneasyTM Mini Kit (Qiagen Inc, Valencia, Calif) and processed according to the manufacturer's instructions. Briefly, a portion of the costal diaphragm (approximately 20 mg) was homogenized with Polytron homogenizer (Kinematica, Inc, Bohemia, NY) and centrifuged at full speed for 3 minutes (4°C) to remove insoluble material if necessary. The sample was added to 2 volumes of 100% ethanol and centrifuged at 10,000*g* for 1 minute until the lysate and ethanol were mixed. Then the sample was added to 1 volume of lysis solution. After transfer of the aqueous phase to a new tube, RNA was precipitated and washed twice with 500 μL to 700 μL wash solution (eg, 75% ethanol). The concentration and purity of the extracted RNA was processed according to the standard protocol. In addition, the high quality of total RNA was determined by capillary electrophoresis with an Agilent bioanalysis system (Bioanalyzer 2001; Agilent Technologies, Inc, Santa Clara, Calif).

Hierarchic Cluster Analysis

Figure 1 shows the hierarchic cluster pattern of the hybridization signal intensities of 3318 probe sets that displayed a coefficient of variation greater than 0.5. In the heat map, the intensity of the color indicates relative expression for each individual gene. The intensity of the color red indicates relative expression greater than the mean for that individual gene, blue indicates expression less than the mean, and the white indicates mean expression. The dendrogram of the clustering is displayed above and is used to identify similarities in expression patterns among the arrays.

Quantitative Real-Time Reverse Transcriptase Polymerase Chain Reaction

The following genes were selected for the validation of the microarray data in this study: cathepsin L1 *(CTSL1),* F-box protein 32 *(FBXO32),* myocyte enhancer factor 2C *(MEF2C),* superoxide dismutase 2 *(SOD2),* and mitochondrial and tripartite motif-containing 63 *(TRIM63).*

The expressions of β_2-microglobulin *(B2M)* and RNA polymerase IIa *(POLR2A)* were used as endogenous controls.

Total RNA was isolated with RNAEasy total RNA isolation kit from Qiagen. Nucleic acid quantification was done on a NanoDrop ND-8000 (NanoDrop Technologies, LLC, Wilmington, Del). Reverse transcription of total RNA (1 μg) to complementary DNA was done with a High Capacity cDNA Reverse Transcription Kit (catalog number 4368813; Applied Biosystems by Life Technologies Corporation, Carlsbad, Calif). In a 0.2-mL polymerase chain reaction tube, 10× reverse transcriptase buffer (2.0 μL), 25× (100 mmol/L) deoxynucleotide triphosphate mix (0.8 μL), 10× reverse transcriptase random primers (2.0 μL), MultiScribe Reverse Transcriptase (2.0 μL; Applied Biosystems), and nuclease-free water were mixed with 1 μg RNA for a total reaction volume of 20 μL. The sample was incubated at 25°C for 10 minutes, 37°C for 120 minutes, and then 85°C for 5 minutes in a DNA Engine Peltier thermal cycler (Bio-Rad Laboratories, Hercules, Calif). Complementary DNA was stored at –20° in a frost-free freezer.

All primers and probes are from Applied Biosystems Assay-on-Demand. Probe is *FAM-NFQ.* Amplification for each target (Table E12) was done in triplicate with each sample, and a no-template control was done for each assay mix. The expressions of β_2-microglobulin *(B2M)* and RNA polymerase IIa *(POLR2A)* were used as endogenous controls. Amplification of complementary DNA that was diluted 10-fold with water was done with 2X Gene Expression Master Mix (catalog number 4369016; Applied Biosystems). In each well of an Optical 96-well Fast Thermal Cycling Plate (catalog number 4346906; Applied Biosystems) was a 20-μL reaction containing 2× Gene Expression Master Mix (10 μL), 20× TaqMan Assay-on-Demand primer and probe mix (1.0 μL), diluted complementary DNA (3.0 μL), and nuclease-free water (6.0 μL). The plate was sealed with MicroAmp Optical Adhesive Film (catalog number 4313663; Applied Biosystems) The sample was incubated at 50°C for 20 minutes, 95°10 minutes, and then 40 cycles of 95°C for 15 seconds and 60°C for 1 minute in a 7900HT real-time polymerase chain reaction thermocycler (Applied Biosystems).

TABLE E1. Functional classification of 779 known genes

Functional categories	Genes	Upregulated
Stress response and redox regulation	86 (11.0%)	80 (93.0%)
Protein turnover and energy metabolism	51 (6.5%)	45 (88.2%)
Muscle specific and neuromuscular	20 (2.6%%)	16 (80.0%)
Transcription regulation	141 (18.1%)	99 (70.2%)
Cell differentiation. growth, and proliferation	16 (2.1%)	15 (93.8%)
Signal transduction	55 (7.1%)	46 (83.6%)
Nuclear metabolism	31 (4.0%)	28 (90.3%)
Extracellular region	137 (17.6%)	108 (78.8%)
Transporter activity	19 (2.4%)	15 (78.9%)
Binding activity	115 (14.8%)	93 (80.9%)
Miscellaneous and unknown	108 (13.9%)	71 (65.7%)

ET/BS

TABLE E2. Expression of stress response and redox regulation genes in the diaphragm during cardiothoracic surgery

Probe set	Symbol	Fold*	*P* value	Description
216598_s_at	*CCL2*	8.2	1.2E–6	Chemokine (C-C motif) ligand 2
204470_at	*CXCL1*	7.4	2.6E–4	Chemokine (C-X-C motif) ligand 1 (melanoma growth-stimulating activity, α)
209774_x_at	*CXCL2*	8.3	1.9E–4	Chemokine (C-X-C motif) ligand 2
207850_at	*CXCL3*	5.1	1.9E–4	Chemokine (C-X-C motif) ligand 3
202859_x_at	*IL8*	22.7	1.1E–3	Interleukin 8
220088_at	*C5AR1*	5.1	1.3E–3	Complement component 5a receptor 1
210390_s_at	*CCL15*	1.7	1.3E–3	Chemokine (C-C motif) ligand 15
823_at	*CX3CL1*	2.7	3.8E–6	Chemokine (C-X3-C motif) ligand 1
205898_at	*CX3CR1*	–2.6	3.1E–3	Chemokine (C-X3-C motif) receptor 1
223454_at	*CXCL16*	2.0	1.4E–3	Chemokine (C-X-C motif) ligand 16
204420_at	*FOSL1*	3.3	6.7E–4	FOS-like antigen 1
205479_s_at	*PLAU*	3.3	1.4E–4	Plasminogen activator, urokinase
210845_s_at	*PLAUR*	4.2	9.8E–5	Plasminogen activator, urokinase receptor
218995_s_at	*EDN1*	1.8	3.1E–3	Endothelin 1
201925_s_at	*CD55*	2.0	3.0E–3	CD55 molecule, decay accelerating factor for complement (Cromer blood group)
212501_at	*CEBPB*	2.2	6.9E–5	CCAAT/enhancer binding protein (C/EBP), β
205419_at	*EBI2*	3.7	1.0E–3	Epstein–Barr virus–induced gene 2 (lymphocyte-specific G protein–coupled receptor)
1555355_a_at	*ETS1*	3.0	1.4E–3	*v-ets* erythroblastosis virus E26 oncogene homolog 1 (avian)
206087_x_at	*HFE*	–1.7	1.7E–3	Hemochromatosis
202948_at	*IL1R1*	2.9	8.5E–4	Interleukin 1 receptor, type I
205403_at	*IL1R2*	6.8	1.9E–3	Interleukin 1 receptor, type II
203574_at	*NFIL3*	4.2	2.1E–3	Nuclear factor, interleukin 3 regulated
201695_s_at	*NP*	6.9	2.5E–6	Nucleoside phosphorylase
206637_at	*P2RY14*	–2.1	2.4E–3	Purinergic receptor P2Y, G-protein coupled, 14
212012_at	*PXDN*	2.5	9.3E–5	Peroxidasin homolog (*Drosophila*)
216834_at	*RGS1*	10.8	1.0E–4	Regulator of G-protein signaling 1
213038_at	*RNF19B*	1.8	4.1E–3	Ring finger protein 19B
202307_s_at	*TAP1*	2.3	9.9E–4	Transporter 1, adenosine triphosphate–binding cassette, subfamily B (*MDR/TAP*)
216920_s_at	*TARP*	–1.8	4.3E–3	T-cell receptor γ alternate reading frame protein
215411_s_at	*TRAF3IP2*	1.7	6.1E–4	*TRAF3*-interacting protein 2
200670_at	*XBP1*	1.6	2.7E–3	X-box binding protein 1
208078_s_at	*ZEB1*	6.0	2.5E–5	Zinc finger E-box binding homeobox 1
1552316_a_at	*GIMAP1*	–1.9	2.5E–4	guanosine triphosphatase, *IMAP* family member 1
210187_at	*FKBP1A*	2.3	3.0E–3	FK506-binding protein 1A, 12 kDa
204908_s_at	*BCL3*	3.9	9.9E–6	B-cell chronic lymphocytic leukemia/lymphoma 3
221009_s_at	*ANGPTL4*	2.6	4.6E–4	Angiopoietin-like 4
200989_at	*HIF1A*	2.6	2.4E–4	Hypoxia-inducible factor 1, α subunit (basic helix-loop-helix transcription factor)
216944_s_at	*ITPR1*	1.6	7.3E–4	Inositol 1,4,5-triphosphate receptor, type 1
204622_x_at	*NR4A2*	3.7	2.7E–3	Nuclear receptor subfamily 4, group A, member 2
203400_s_at	*TF*	1.4	4.2E–3	Transferrin
209112_at	*CDKN1B*	–1.6	5.0E–3	Cyclin-dependent kinase inhibitor 1B (p27, Kip1)
221031_s_at	*APOLD1*	5.6	2.0E–5	Apolipoprotein L domain containing 1
204748_at	*PTGS2*	5.2	4.0E–4	Prostaglandin–endoperoxide synthase 2 (prostaglandin G/H synthase and cyclooxygenase)
221477_s_at	*MGC5618*	1.6	4.3E–3	Hypothetical protein MGC5618
205548_s_at	*BTG3*	2.6	1.6E–4	*BTG* family, member 3
200878_at	*EPAS1*	1.5	3.2E–3	Endothelial *PAS* domain protein 1
202912_at	*ADM*	3.6	2.6E–4	Adrenomedullin
209682_at	*CBLB*	1.8	1.9E–3	Cas-Br-M (murine) ecotropic retroviral transforming sequence b
223377_x_at	*CISH*	6.8	5.0E–7	Cytokine-inducible SH2-containing protein
207442_at	*CSF3*	2.7	9.7E–6	Colony-stimulating factor 3 (granulocyte)
205207_at	*IL6*	15.6	3.5E–5	Interleukin 6 (interferon, β2)
212196_at	*IL6ST*	2.0	2.1E–3	Interleukin 6 signal transducer (glycoprotein 130, oncostatin M receptor)
1552611_a_at	*JAK1*	1.5	4.3E–3	Janus kinase 1 (a protein tyrosine kinase)
202431_s_at	*MYC*	8.0	5.2E–5	*v-myc* myelocytomatosis viral oncogene homolog (avian)
211580_s_at	*PIK3R3*	2.8	6.8E–4	Phosphoinositide-3-kinase, regulatory subunit 3 (p55, γ)

(Continued)

TABLE E2. Continued

Probe set	Symbol	Fold*	*P* value	Description
209193_at	*PIM1*	3.5	2.5E–5	Pim-1 oncogene
202327_s_at	*PKD1*	2.0	3.3E–4	Polycystic kidney disease 1 (autosomal dominant)
210001_s_at	*SOCS1*	4.7	1.0E–6	Suppressor of cytokine signaling 1
203372_s_at	*SOCS2*	3.1	2.7E–5	Suppressor of cytokine signaling 2
227697_at	*SOCS3*	9.4	1.1E–5	Suppressor of cytokine signaling 3
226837_at	*SPRED1*	2.2	2.2E–3	Sprouty-related, *EVH1* domain containing 1
212558_at	*SPRY1*	1.7	2.9E–3	Sprouty homolog 1, antagonist of fibroblast growth factor signaling (*Drosophila*)
208992_s_at	*STAT3*	1.6	2.0E–3	Signal transducer and activator of transcription 3 (acute-phase response factor)
232768_at	*CCNB2*	1.5	2.3E–3	Cyclin B2
204252_at	*CDK2*	1.6	1.9E–3	Cyclin-dependent kinase 2
202284_s_at	*CDKN1A*	4.9	7.0E–7	Cyclin-dependent kinase inhibitor 1A (p21, Cip1)
203725_at	*GADD45A*	3.0	4.5E–4	Growth arrest and DNA damage–inducible, α
209305_s_at	*GADD45B*	10.2	5.3E–6	Growth arrest and DNA damage–inducible, β
204121_at	*GADD45G*	4.3	1.8E–6	Growth arrest and DNA damage–inducible, γ
204286_s_at	*PMAIP1*	2.8	2.9E–3	Phorbol-12-myristate-13-acetate–induced protein 1
202628_s_at	*SERPINE1*	8.6	3.8E–4	Serpin peptidase inhibitor, clade E (nexin, plasminogen activator inhibitor type 1), member 1
235086_at	*THBS1*	8.2	1.5E–5	Thrombospondin 1
209295_at	*TNFRSF10B*	2.5	4.9E–5	Tumor necrosis factor receptor superfamily, member 10b
238624_at	*NLK*	1.4	4.1E–3	NF κB essential modulator–like kinase
242751_at	*PRDX6*	1.9	6.3E–4	Peroxiredoxin 6
215223_s_at	*SOD2*	2.9	1.1E–5	Superoxide dismutase 2, mitochondrial
208864_s_at	*TXN*	1.9	2.9E–3	Thioredoxin
223209_s_at	*SELS*	1.5	4.0E–3	Selenoprotein S
212859_x_at	*MT1E*	3.5	9.3E–6	Metallothionein 1E
213629_x_at	*MT1F*	3.6	4.9E–5	Metallothionein 1J (pseudogene)
204745_x_at	*MT1G*	3.5	8.1E–6	Metallothionein 1G
206461_x_at	*MT1H*	3.4	2.8E–5	Metallothionein 1H
217546_at	*MT1M*	11.4	6.0E–7	Metallothionein 1M
211456_x_at	*MT1P2*	3.2	5.2E–5	Metallothionein 1 pseudogene 2
208581_x_at	*MT1X*	3.3	8.3E–5	Metallothionein 1X
212185_x_at	*MT2A*	2.4	1.5E–5	Metallothionein 2A

**Fold* denotes fold change between presurgical and postsurgical conditions.

TABLE E3. Expression of protein turnover and energy metabolism genes in the diaphragm during cardiothoracic surgery

Probe set	Symbol	Fold*	*P* value	Description
200881_s_at	*DNAJA1*	1.9	2.9E–3	DnaJ (heat shock protein 40) homolog, subfamily A, member 1
200664_s_at	*DNAJB1*	2.8	3.6E–3	DnaJ (heat shock protein 40) homolog, subfamily B, member 1
208810_at	*DNAJB6*	1.7	4.0E–4	DnaJ (heat shock protein 40) homolog, subfamily B, member 6
201041_s_at	*DUSP1*	3.7	8.8E–4	Dual specificity phosphatase 1
218459_at	*TOR3A*	2.0	2.2E–4	Torsin family 3, member A
225647_s_at	*CTSC*	2.7	2.1E–3	Cathepsin C
202087_s_at	*CTSL1*	2.0	2.8E–3	Cathepsin L1
201502_s_at	*NFKBIA*	3.7	1.4E–6	Nuclear factor of κ light polypeptide gene enhancer in B-cells inhibitor, α
223217_s_at	*NFKBIZ*	3.9	8.1E–5	Nuclear factor of κ light polypeptide gene enhancer in B-cells inhibitor, ζ
202723_s_at	*FOXO1*	1.9	2.0E–3	Forkhead box O1
204131_s_at	*FOXO3*	1.7	2.0E–3	Forkhead box O3
236975_at	*USP12*	1.8	7.2E–4	Ubiquitin-specific peptidase 12
231990_at	*USP15*	2.2	1.5E–4	Ubiquitin-specific peptidase 15
220370_s_at	*USP36*	1.9	2.4E–4	Ubiquitin-specific peptidase 36
233327_at	C6orf157	1.5	2.2E–3	Chromosome 6 open reading frame 157
241762_at	*FBXO32*	–3.5	5.6E–5	F-box protein 32
236972_at	*TRIM63*	2.6	4.1E–5	Tripartite motif-containing 63
243046_at	*UBE2D3*	1.8	7.1E–4	Ubiquitin-conjugating enzyme E2D 3 (UBC4/5 homolog, yeast)
65521_at	*UBE2D4*	1.5	4.2E–3	Ubiquitin-conjugating enzyme E2D 4 (putative)
222435_s_at	*UBE2J1*	1.7	2.3E–4	Ubiquitin-conjugating enzyme E2, J1 (UBC6 homolog, yeast)
202779_s_at	*UBE2S*	1.6	1.1E–3	Ubiquitin-conjugating enzyme E2S
225954_s_at	*MIDN*	4.3	1.3E–6	Midnolin
223481_s_at	*MRPL47*	–1.8	8.9E–4	Mitochondrial ribosomal protein L47
1555878_at	*RPS24*	2.4	1.2E–4	Ribosomal protein S24
238156_at	*RPS6*	2.4	7.6E–5	Ribosomal protein S6
225827_at	*EIF2C2*	1.7	1.5E–3	Eukaryotic translation initiation factor 2C, 2
208624_s_at	*EIF4G1*	1.6	2.0E–3	Eukaryotic translation initiation factor 4 γ, 1
1554309_at	*EIF4G3*	1.9	3.9E–4	Eukaryotic translation initiation factor 4 γ, 3
208707_at	*EIF5*	1.9	1.7E–4	Eukaryotic translation initiation factor 5
201574_at	*ETF1*	1.8	3.0E–3	Eukaryotic translation termination factor 1
224873_s_at	*MRPS25*	–1.4	5.0E–3	Mitochondrial ribosomal protein S25
224692_at	*PPP1R15B*	2.1	9.0E–5	Protein phosphatase 1, regulatory (inhibitor) subunit 15B
201101_s_at	*BCLAF1*	1.5	3.6E–3	*BCL2*-associated transcription factor 1
205681_at	*BCL2A1*	11.3	3.8E–3	*BCL2*-related protein A1
209189_at	*FOS*	6.8	1.9E–3	*v-fos* FBJ murine osteosarcoma viral oncogene homolog
201473_at	*JUNB*	4.1	2.6E–5	B-*jun* proto-oncogene
200796_s_at	*MCL1*	3.0	4.4E–6	Myeloid cell leukemia sequence 1 (*BCL2*-related)
202340_x_at	*NR4A1*	3.7	2.6E–3	Nuclear receptor subfamily 4, group A, member 1
209959_at	*NR4A3*	4.6	1.1E–4	Nuclear receptor subfamily 4, group A, member 3
213572_s_at	*SERPINB1*	2.8	2.1E–3	Serpin peptidase inhibitor, clade B (ovalbumin), member 1
211527_x_at	*VEGFA*	1.8	3.9E–3	Vascular endothelial growth factor A
210287_s_at	*FLT1*	3.5	8.1E–4	fms-related tyrosine kinase 1 (vascular endothelial growth factor/vascular permeability factor receptor)
240187_at	*PPP1R3C*	–2.8	1.3E–4	Protein phosphatase 1, regulatory (inhibitor) subunit 3C
209184_s_at	*IRS2*	2.0	3.8E–4	Insulin receptor substrate 2
205960_at	*PDK4*	4.0	3.5E–3	Pyruvate dehydrogenase kinase, isozyme 4
235374_at	*MDH1*	–2.2	2.3E–3	Malate dehydrogenase 1, nicotinamide adenine dinucleotide (soluble)
206932_at	*CH25H*	8.6	1.4E–5	Cholesterol 25-hydroxylase
243296_at	*PBEF1*	5.1	3.3E–4	Pre–B-cell colony-enhancing factor 1
208383_s_at	*PCK1*	–2.3	1.3E–3	Phosphoenolpyruvate carboxykinase 1 (soluble)
216236_s_at	*SLC2A3*	5.1	1.1E–5	Solute carrier family 2 (facilitated glucose transporter), member 3
201195_s_at	*SLC7A5*	2.2	1.1E–3	Solute carrier family 7 (cationic amino acid transporter, y+ system), member 5

**Fold* denotes fold change between presurgical and postsurgical conditions.

TABLE E4. Expression of transcript regulation genes in the diaphragm during cardiothoracic surgery

Probe set	Symbol	Fold*	*P* value	Description
Negative regulation of transcription				
201862_s_at	*LRRFIP1*	2.1	2.9E–3	Leucine-rich repeat (in *FLII*) interacting protein 1
202861_at	*PER1*	2.5	1.5E–4	Period homolog 1 (*Drosophila*)
203749_s_at	*RARA*	1.9	2.5E–3	Retinoic acid receptor, alpha
222815_at	*RNF12*	2.1	9.8E–4	Ring finger protein 12
202241_at	*TRIB1*	3.3	2.0E–4	Tribbles homolog 1 (*Drosophila*)
213183_s_at	*CDKN1C*	–1.7	5.0E–3	Cyclin-dependent kinase inhibitor 1C (p57, Kip2)
227404_s_at	*EGR1*	3.0	6.0E–4	Early growth response 1
202768_at	*FOSB*	5.2	1.2E–3	FBJ murine osteosarcoma viral oncogene homolog B
237403_at	*GFI1B*	2.2	2.3E–5	Growth factor independent 1B (potential regulator of *CDKN1A,* translocated in *CML*)
203395_s_at	*HES1*	2.8	3.0E–3	Hairy and enhancer of split 1 (*Drosophila*)
203275_at	*IRF2*	–1.6	4.1E–3	Interferon regulatory factor 2
203297_s_at	*JARID2*	1.6	1.1E–3	Jumonji, AT-rich interactive domain 2
213146_at	*JMJD3*	4.3	2.4E–4	Jumonji domain containing 3
202393_s_at	*KLF10*	2.8	1.6E–4	Kruppel-like factor 10
205932_s_at	*MSX1*	1.9	2.3E–3	msh homeobox 1
221715_at	*MYST3*	1.7	2.2E–3	*MYST* histone acetyltransferase (monocytic leukemia) 3
215073_s_at	*NR2F2*	–1.9	4.5E–4	Nuclear receptor subfamily 2, group F, member 2
210391_at	*NR6A1*	1.4	2.5E–3	Nuclear receptor subfamily 6, group A, member 1
202600_s_at	*NRIP1*	2.1	7.7E–5	Nuclear receptor interacting protein 1
228964_at	*PRDM1*	2.7	1.4E–4	*PR* domain containing 1, with *ZNF* domain
201846_s_at	*RYBP*	2.4	3.6E–4	*RING1* and *YY1* binding protein
204900_x_at	*SAP30*	1.6	2.9E–3	Sin3A-associated protein, 30 kDa
203313_s_at	*TGIF1*	4.1	1.7E–4	Transforming growth factor β–induced factor homeobox 1
213138_at	*ARID5A*	2.2	2.1E–3	AT-rich interactive domain 5A (MRF1-like)
1558000_at	*ARID5B*	3.1	2.4E–5	AT-rich interactive domain 5B (MRF1-like)
201277_s_at	*HNRPAB*	1.9	2.7E–3	Heterogeneous nuclear ribonucleoprotein A/B
208930_s_at	*ILF3*	1.4	4.6E–3	Interleukin enhancer binding factor 3, 90 kDa
221841_s_at	*KLF4*	3.1	3.1E–4	Kruppel-like factor 4 (gut)
223467_at	*RASD1*	5.7	3.1E–5	*RAS,* dexamethasone-induced 1
Positive regulation of transcription				
205290_s_at	*BMP2*	3.8	2.0E–5	Bone morphogenetic protein 2
200033_at	*DDX5*	1.8	3.0E–4	*DEAD* (Asp-Glu-Ala-Asp) box polypeptide 5
1567013_at	*NFE2L2*	1.9	9.2E–4	Nuclear factor (erythroid-derived 2)–like 2
211951_at	*NOLC1*	2.0	7.5E–4	Nucleolar and coiled-body phosphoprotein 1
223394_at	*SERTAD1*	3.0	1.7E–3	*SERTA* domain containing 1
206170_at	*ADRB2*	1.8	3.3E–3	Adrenergic, beta-2-, receptor, surface
225557_at	*AXUD1*	6.4	8.9E–5	*AXIN1* upregulated 1
204093_at	*CCNH*	1.7	3.0E–4	Cyclin H
212418_at	*ELF1*	1.8	3.4E–3	E74-like factor 1 (ets domain transcription factor)
1553613_s_at	*FOXC1*	2.6	4.6E–5	Forkhead box C1
202531_at	*IRF1*	4.5	2.6E–4	Interferon regulatory factor 1
224606_at	*KLF6*	2.8	8.5E–6	Kruppel-like factor 6
209348_s_at	*MAF*	–1.7	3.2E–3	*v-maf* musculoaponeurotic fibrosarcoma oncogene homolog (avian)
218559_s_at	*MAFB*	2.6	1.1E–4	*v-maf* musculoaponeurotic fibrosarcoma oncogene homolog B (avian)
205135_s_at	*NUFIP1*	1.9	8.8E–4	Nuclear fragile X mental retardation protein interacting protein 1
236557_at	*ZBTB38*	1.6	1.7E–3	Zinc finger and *BTB* domain containing 38
201329_s_at	*ETS2*	4.9	1.8E–5	*v-ets* erythroblastosis virus E26 oncogene homolog 2 (avian)
200750_s_at	*RAN*	1.5	2.5E–3	RAN, member *RAS* oncogene family
206036_s_at	*REL*	1.8	1.6E–3	*v-rel* reticuloendotheliosis viral oncogene homolog (avian)
Regulation of transcription				
213198_at	*ACVR1B*	1.7	3.3E–4	Activin A receptor, type IB
203322_at	*ADNP2*	1.6	9.8E–4	*ADNP* homeobox 2
1560765_a_at	*ARHGAP22*	1.9	6.3E–4	Rho guanosine triphosphatase activating protein 22
244519_at	*ASXL1*	1.7	9.7E–4	Additional sex combs–like 1 (*Drosophila*)

(Continued)

TABLE E4. Continued

Probe set	Symbol	Fold*	*P* value	Description
204194_at	*BACH1*	1.9	1.3E–3	*BTB* and *CNC* homology 1, basic leucine zipper transcription factor 1
1559975_at	*BTG1*	2.3	3.1E–4	B-cell translocation gene 1, antiproliferative
201235_s_at	*BTG2*	6.0	4.5E–4	*BTG* family, member 2
200777_s_at	*BZW1*	1.6	1.1E–3	Basic leucine zipper and W2 domains 1
1555411_a_at	*CCNL1*	4.2	1.7E–6	Cyclin L1
213006_at	*CEBPD*	5.0	1.0E–6	CCAAT/enhancer binding protein (C/EBP), δ
207630_s_at	*CREM*	3.3	3.0E–5	Cyclic adenosine monophosphate–responsive element modulator
224654_at	*DDX21*	2.9	7.7E–4	*DEAD* (Asp-Glu-Ala-Asp) box polypeptide 21
202776_at	*DNTTIP2*	1.8	3.9E–3	Deoxynucleotidyltransferase, terminal, interacting protein 2
226952_at	*EAF1*	1.5	2.7E–3	ELL-associated factor 1
226099_at	*ELL2*	7.3	3.2E–5	Elongation factor, RNA polymerase II, 2
203643_at	*ERF*	1.5	4.2E–3	Ets2 repressor factor
1561167_at	*ETV6*	2.1	5.3E–4	Ets variant gene 6 (*TEL* oncogene)
241824_at	*FOSL2*	2.3	5.2E–4	FOS-like antigen 2
218458_at	*GMCL1*	–1.6	2.2E–3	Germ cell–less homolog 1 (*Drosophila*)
222830_at	*GRHL1*	2.3	2.5E–4	Grainyhead-like 1 (*Drosophila*)
208066_s_at	*GTF2B*	1.6	1.8E–3	General transcription factor IIB
213844_at	*HOXA5*	–2.0	1.7E–3	Homeobox A5
205453_at	*HOXB2*	–1.6	9.9E–4	Homeobox B2
228904_at	*HOXB3*	–1.7	2.4E–3	Homeobox B3
229732_at	*HSZFP36*	–1.9	4.1E–4	*ZFP36* for a zinc finger protein
1557174_a_at	*IRAK1BP1*	–2.0	8.0E–4	Interleukin 1 receptor–associated kinase 1 binding protein 1
224569_s_at	*IRF2BP2*	1.5	3.0E–3	Interferon regulatory factor 2 binding protein 2
224933_s_at	*JMJD1C*	2.1	2.7E–3	Jumonji domain containing 1C
212723_at	*JMJD6*	2.1	4.6E–4	Jumonji domain containing 6
222728_s_at	*JOSD3*	1.8	1.0E–3	Josephin domain containing 3
Regulation of transcription				
208989_s_at	*KDM2A*	1.5	3.6E–3	F-box and leucine-rich repeat protein 11
1556060_a_at	*KIAA1702*	1.8	1.7E–3	KIAA1702 protein
203542_s_at	*KLF9*	2.6	4.7E–5	Kruppel-like factor 9
200704_at	*LITAF*	3.2	2.8E–3	Lipopolysaccharide-induced tumor necrosis factor
200776_s_at	*LOC151579*	2.0	5.5E–4	Similar to basic leucine zipper and W2 domains 1
244818_at	*LOC390933*	–1.8	4.4E–3	Similar to hypothetical protein
36711_at	*MAFF*	8.7	4.0E–7	*v-maf* musculoaponeurotic fibrosarcoma oncogene homolog F (avian)
226206_at	*MAFK*	1.5	2.2E–3	*v-maf* musculoaponeurotic fibrosarcoma oncogene homolog K (avian)
227538_at	*MED26*	1.6	2.3E–3	Mediator complex subunit 26
1552330_at	*MGC16385*	–1.6	7.5E–4	Hypothetical protein MGC16385
225344_at	*NCOA7*	1.9	4.9E–3	Nuclear receptor coactivator 7
210162_s_at	*NFATC1*	1.5	3.4E–3	Nuclear factor of activated T cells, cytoplasmic, calcineurin-dependent 1
241797_at	*NFIX*	–1.5	3.2E–3	Nuclear factor I/X (CCAAT-binding transcription factor)
209706_at	*NKX3-1*	1.7	1.0E–3	*NK3* homeobox 1
205251_at	*PER2*	1.9	2.9E–3	Period homolog 2 (*Drosophila*)
209034_at	*PNRC1*	1.8	1.9E–3	Proline-rich nuclear receptor coactivator 1
215281_x_at	*POGZ*	–1.5	2.3E–3	Pogo transposable element with ZNF domain
203737_s_at	*PPRC1*	3.3	2.0E–5	Peroxisome proliferator-activated receptor γ, coactivator-related 1
208965_s_at	*PYHIN1*	3.0	8.8E–4	Pyrin and *HIN* domain family, member 1
201586_s_at	*SFPQ*	2.5	6.4E–4	Splicing factor proline/glutamine-rich (polypyrimidine tract binding protein associated)
220358_at	*SNFT*	1.5	2.2E–3	Jun dimerization protein p21SNFT
219993_at	*SOX17*	4.1	3.2E–4	*SRY* (sex determining region Y)–box 17
221213_s_at	*SUHW4*	–2.1	4.7E–3	Suppressor of hairy wing homolog 4 (*Drosophila*)
1554415_at	*TAF5L*	1.9	6.7E–4	TAF5-like RNA polymerase II, p300/CBP–associated factor (PCAF)–associated factor, 65 kDa
238346_s_at	*TGS1*	1.6	3.1E–3	Trimethylguanosine synthase homolog (*Saccharomyces cerevisiae*)
229983_at	*TIGD2*	–1.6	1.9E–3	Tigger transposable element derived 2
215111_s_at	*TSC22D1*	1.6	2.7E–3	*TSC22* domain family, member 1

(Continued)

TABLE E4. Continued

Probe set	Symbol	Fold*	*P* value	Description
Regulation of transcription				
1554036_at	*ZBTB24*	2.3	3.6E–4	Zinc finger and *BTB* domain containing 24
227162_at	*ZBTB26*	–1.6	3.0E–3	Zinc finger and *BTB* domain containing 26
206098_at	*ZBTB6*	–1.5	1.6E–3	Zinc finger and *BTB* domain containing 6
207090_x_at	*ZFP30*	–1.5	3.9E–3	Zinc finger protein 30 homolog (mouse)
216960_s_at	*ZNF133*	–1.4	4.3E–3	Zinc finger protein 133
219854_at	*ZNF14*	–1.5	3.2E–3	Zinc finger protein 14
206314_at	*ZNF167*	–1.9	3.4E–4	Zinc finger protein 167
219495_s_at	*ZNF180*	–1.6	7.4E–4	Zinc finger protein 180
213218_at	*ZNF187*	–1.6	6.5E–4	Zinc finger protein 187
233461_x_at	*ZNF226*	–1.6	1.3E–3	Zinc finger protein 226
242919_at	*ZNF253*	–1.8	1.6E–3	Zinc finger protein 253
1558700_s_at	*ZNF260*	–1.9	3.2E–4	Zinc finger protein 260
1562991_at	*ZNF292*	1.9	4.5E–4	Zinc finger protein 292
233952_s_at	*ZNF295*	2.5	2.6E–4	Zinc finger protein 295
227613_at	*ZNF331*	3.6	4.3E–4	Zinc finger protein 331
228927_at	*ZNF397*	–1.6	8.0E–4	Zinc finger protein 397
209944_at	*ZNF410*	1.6	3.3E–3	Zinc finger protein 410
205514_at	*ZNF415*	–1.6	3.2E–3	Zinc finger protein 415
1562211_a_at	*ZNF491*	1.7	1.3E–3	Zinc finger protein 491
1553957_at	*ZNF564*	–1.8	6.7E–4	Zinc finger protein 564
1553696_s_at	*ZNF569*	–1.8	3.4E–3	Zinc finger protein 569
217627_at	*ZNF573*	–1.6	3.3E–3	Zinc finger protein 573
235690_at	*ZNF594*	–1.7	3.7E–3	Zinc finger protein 594
239007_at	*ZNF616*	–1.6	5.0E–3	Zinc finger protein 616
206188_at	*ZNF623*	–1.8	3.0E–3	Zinc finger protein 623
232272_at	*ZNF624*	–1.9	1.4E–3	Zinc finger protein 624
224492_s_at	*ZNF627*	–1.7	2.6E–3	Zinc finger protein 627
231950_at	*ZNF658*	–2.1	2.5E–3	Zinc finger protein 658
232563_at	*ZNF684*	–1.5	2.2E–3	Zinc finger protein 684
1554770_x_at	*ZNF785*	–1.8	3.2E–3	Zinc finger protein 785
235170_at	*ZNF92*	–1.5	2.0E–3	Zinc finger protein 92
204258_at	*CHD1*	2.8	2.7E–4	Zhromodomain helicase DNA-binding protein 1
218880_at	*FOSL2*	3.3	2.1E–6	FOS-like antigen 2
219351_at	*TRAPPC2*	–1.7	4.2E–3	Trafficking protein particle complex 2
204094_s_at	*TSC22D2*	2.2	1.2E–3	*TSC22* domain family, member 2
200828_s_at	*ZNF207*	1.5	2.2E–3	Zinc finger protein 207

**Fold* denotes fold change between presurgical and postsurgical conditions.

TABLE E5. Expression of cell proliferation, growth, and differentiation genes in the diaphragm during cardiothoracic surgery

Probe set	Symbol	Fold*	*P* value	Description
Cell growth				
213895_at	EMP1	3.8	1.5E–5	Epithelial membrane protein 1
218088_s_at	RRAGC	1.6	2.0E–3	Ras-related guanosine triphosphate–binding C
232541_at	EGFR	2.3	1.5E–4	Epidermal growth factor receptor (erythroblastic leukemia viral (*v-erb-b*) oncogene homolog, avian)
Negative regulation of cell growth				
212099_at	RHOB	3.0	1.3E–5	*ras* homolog gene family, member B
203120_at	TP53BP2	1.8	4.8E–3	Tumor protein p53 binding protein, 2
1555608_at	CAPRIN2	1.7	8.6E–4	Caprin family member 2
239648_at	DCUN1D3	2.4	4.1E–5	*DCN1,* defective in cullin neddylation 1, domain containing 3 (*Saccharomyces cerevisiae*)
Positive regulation of cell growth				
205302_at	IGFBP1	1.6	4.4E–3	Insulin-like growth factor binding protein 1
Regulation of cell cycle				
203625_x_at	SKP2	–1.8	6.9E–4	S-phase kinase-associated protein 2 (p45)
202286_s_at	TACSTD2	2.6	6.8E–4	Tumor-associated calcium signal transducer 2
217523_at	CD44	2.9	5.0E–4	CD44 molecule (Indian blood group)
Regulation of cell growth				
209101_at	CTGF	2.8	1.7E–5	Connective tissue growth factor
209074_s_at	FAM107A	3.4	1.7E–5	Family with sequence similarity 107, member A
201830_s_at	NET1	3.0	4.6E–4	Neuroepithelial cell transforming gene 1
233223_at	NEDD9	1.7	5.1E–4	Neural precursor cell expressed, developmentally downregulated 9
Enhances DNA synthesis and may play a role in cell proliferation				
228266_s_at	HDGFRP3	1.9	2.3E–4	Hepatoma-derived growth factor, related protein 3

**Fold* denotes fold change between presurgical and postsurgical conditions.

TABLE E6. Expression of signal transduction genes in the diaphragm during cardiothoracic surgery

Probe set	Symbol	Fold*	*P* value	Description
Cell surface receptor linked signal transduction				
240221_at	*CSNK1A1*	1.6	4.2E–3	Casein kinase 1, α 1
212951_at	*GPR116*	1.5	4.0E–3	G-protein–coupled receptor 116
212070_at	*GPR56*	2.0	1.8E–3	G-protein–coupled receptor 56
204597_x_at	*STC1*	7.8	2.5E–4	Stanniocalcin 1
Negative regulation of Rho protein signal transduction				
210762_s_at	*DLC1*	1.8	9.2E–4	Deleted in liver cancer 1
209324_s_at	*RGS16*	4.5	2.2E–4	Regulator of G-protein signaling 16
202388_at	*RGS2*	5.4	1.4E–4	Regulator of G-protein signaling 2, 24 kDa
224390_s_at	*RGS8*	1.9	3.6E–3	Regulator of G-protein signaling 8
223169_s_at	*RHOU*	2.8	3.9E–5	Ras homolog gene family, member U
Rac protein signal transduction				
201461_s_at	*MAPKAPK2*	1.6	1.6E–3	Mitogen-activated protein kinase–activated protein kinase 2
209050_s_at	*RALGDS*	2.0	1.3E–4	Ral guanine nucleotide dissociation stimulator
226122_at	*PLEKHG1*	2.7	7.5E–5	Pleckstrin homology domain containing, family G (with RhoGef domain) member 1
Regulation of signal transduction				
227481_at	*CNKSR3*	2.2	8.3E–5	*CNKSR* family member 3
214721_x_at	*CDC42EP4*	2.6	8.2E–6	CDC42 effector protein (Rho guanosine triphosphatase binding) 4
1555730_a_at	*CFL1*	1.6	1.6E–3	Cofilin 1 (nonmuscle)
229218_at	*COL1A2*	–2.2	3.3E–3	Collagen, type I, alpha 2
212935_at	*MCF2L*	2.0	4.2E–3	MCF.2 cell line-derived transforming sequence–like
Signal transduction				
231907_at	*ABL2*	2.0	2.3E–3	*v-abl* Abelson murine leukemia viral oncogene homolog 2 (arg, Abelson-related gene)
210517_s_at	*AKAP12*	2.4	4.6E–3	A kinase (*PRKA*) anchor protein (gravin) 12
228176_at	C9orf47	2.8	2.1E–4	Chromosome 9 open reading frame 47
Rho protein signal transduction				
209287_s_at	*CDC42EP3*	1.5	3.0E–3	CDC42 effector protein (Rho guanosine triphosphatase binding) 3
218157_x_at	*CDC42SE1*	2.2	1.3E–3	CDC42 small effector 1
203104_at	*CSF1R*	–1.8	1.4E–3	Colony-stimulating factor 1 receptor, formerly McDonough feline sarcoma viral (*v-fms*) oncogene homolog
207945_s_at	*CSNK1D*	2.4	5.9E–4	Casein kinase 1, delta
208335_s_at	DARC	2.7	1.7E–4	Duffy blood group, chemokine receptor
227692_at	*GNAI1*	–1.7	1.4E–3	Guanine nucleotide binding protein (G protein), α inhibiting activity polypeptide 1
223620_at	*GPR34*	–2.3	3.7E–4	G-protein–coupled receptor 34
228263_at	*GRASP*	2.2	4.6E–5	*GRP1* (general receptor for phosphoinositides 1)–associated scaffold protein
233953_at	*GUCA1C*	2.1	9.6E–4	Guanylate cyclase activator 1C
211676_s_at	*IFNGR1*	1.9	3.4E–4	Interferon γ receptor 1
230550_at	*MS4A6A*	–1.7	1.2E–3	Membrane-spanning 4-domains, subfamily A, member 6A
202149_at	*NEDD9*	2.3	7.3E–4	Neural precursor cell expressed, developmentally downregulated 9
207075_at	*NLRP3*	2.4	1.3E–3	*NLR* family, pyrin domain containing 3
217302_at	*OR2F2*	1.5	4.3E–3	Olfactory receptor, family 2, subfamily F, member 2
203708_at	*PDE4B*	2.6	3.5E–4	Phosphodiesterase 4B, cyclic adenosine monophosphate–specific (phosphodiesterase E4 dunce homolog, *Drosophila*)
238419_at	*PHLDB2*	2.0	1.3E–4	Pleckstrin homology–like domain, family B, member 2
219155_at	*PITPNC1*	2.2	2.0E–3	Phosphatidylinositol transfer protein, cytoplasmic 1
215894_at	*PTGDR*	–1.6	3.4E–3	Prostaglandin D2 receptor (DP)
202716_at	*PTPN1*	2.2	3.4E–3	Protein tyrosine phosphatase, nonreceptor type 1
208370_s_at	*RCAN1*	1.7	9.6E–4	Regulator of calcineurin 1
209941_at	*RIPK1*	1.9	1.3E–3	Receptor (TNFRSF)–interacting serine–threonine kinase-1
209723_at	*SERPINB9*	2.0	1.7E–3	Serpin peptidase inhibitor, clade B (ovalbumin), member 9
214597_at	*SSTR2*	1.5	4.6E–3	Somatostatin receptor 2
206026_s_at	*TNFAIP6*	4.1	8.6E–5	Tumor necrosis factor α–induced protein 6
227345_at	*TNFRSF10D*	2.9	2.9E–5	Tumor necrosis factor receptor superfamily, member 10d, decoy with truncated death domain
224553_s_at	*TNFRSF18*	–1.6	2.8E–3	Tumor necrosis factor receptor superfamily, member 18
202871_at	*TRAF4*	1.5	2.5E–3	Tumor necrosis factor receptor–associated factor 4

(Continued)

ET/BS

TABLE E6. Continued

Probe set	Symbol	Fold*	*P* value	Description
213476_x_at	*TUBB3*	1.7	9.3E–4	Tubulin, β 3
213425_at	*WNT5A*	–2.0	6.6E–4	Wingless-type MMTV integration site family, member 5A
200641_s_at	*YWHAZ*	1.5	1.7E–3	Tyrosine 3-monooxygenase/tryptophan 5-monooxygenase activation protein, ζ polypeptide
Small guanosine triphosphatase–mediated signal transduction				
203586_s_at	*ARL4D*	1.6	1.1E–3	adenosine diphosphate ribosylation factor–like 4D
242727_at	*ARL5B*	1.5	2.8E–3	adenosine diphosphate ribosylation factor–like 5B
219622_at	*RAB20*	1.9	5.9E–4	RAB20, member *RAS* oncogene family
221014_s_at	*RAB33B*	–1.6	2.7E–3	RAB33B, member *RAS* oncogene family
212724_at	*RND3*	3.7	2.5E–6	Rho family guanosine triphosphatase 3

**Fold* denotes fold change between presurgical and postsurgical conditions.

TABLE E7. Expression of nuclei metabolism genes in the diaphragm during cardiothoracic surgery

Probe set	Symbol	Fold*	*P* value	Description
DNA replication				
204510_at	*CDC7*	1.9	1.1E–4	Cell division cycle 7 homolog (*Saccharomyces cerevisiae*)
201970_s_at	*NASP*	1.7	8.8E–4	Nuclear autoantigenic sperm protein (histone-binding)
238992_at	*POLI*	–2.1	4.9E–4	Polymerase (DNA-directed) ι
207266_x_at	*RBMS1*	1.5	3.1E–3	RNA-binding motif, single-stranded interacting protein 1
208900_s_at	*TOP1*	2.3	8.6E–4	Topoisomerase (DNA) I
Messenger RNA processing				
226153_s_at	*CNOT6L*	1.5	2.7E–3	*CCR4-NOT* transcription complex, subunit 6–like
201055_s_at	*HNRNPA*0	1.7	2.5E–3	Heterogeneous nuclear ribonucleoprotein A0
212028_at	*RBM25*	1.6	1.4E–3	RNA-binding motif protein 25
Positive regulation of DNA replication				
205239_at	*AREG*	5.7	2.9E–3	Amphiregulin (schwannoma-derived growth factor)
218718_at	*PDGFC*	–1.6	4.2E–3	Platelet-derived growth factor C
RNA splicing				
201386_s_at	*DHX15*	1.6	3.2E–3	*DEAH* (Asp-Glu-Ala-His) box polypeptide 15
201303_at	*EIF4A3*	2.1	8.4E–5	Eukaryotic translation initiation factor 4A, isoform 3
227110_at	*HNRNPC*	1.5	4.6E–3	Heterogeneous nuclear ribonucleoprotein C (C1/C2)
201376_s_at	*HNRPF*	1.6	2.3E–3	Heterogeneous nuclear ribonucleoprotein F
244235_at	*IVNS1ABP*	4.8	3.7E–5	Influenza virus NS1A binding protein
222040_at	*LOC728844*	1.6	8.7E–4	Hypothetical protein LOC728844
202189_x_at	*PTBP1*	2.0	8.8E–4	Polypyrimidine tract–binding protein 1
222443_s_at	*RBM8A*	1.8	4.0E–4	RNA-binding motif protein 8A
201070_x_at	*SF3B1*	1.5	1.8E–3	Splicing factor 3b, subunit 1, 155 kDa
200892_s_at	*SFRS10*	1.8	5.6E–4	Splicing factor, arginine/serine-rich 10 (transformer 2 homolog, *Drosophila*)
200754_x_at	*SFRS2*	1.6	3.3E–3	Splicing factor, arginine/serine-rich 2
206108_s_at	*SFRS6*	1.6	1.1E–3	Splicing factor, arginine/serine-rich 6
213649_at	*SFRS7*	1.6	1.6E–3	Splicing factor, arginine/serine-rich 7, 35k Da
213175_s_at	*SNRPB*	1.6	2.1E–3	Small nuclear ribonucleoprotein polypeptides B and B1
209024_s_at	*SYNCRIP*	1.8	5.0E–4	Synaptotagmin-binding, cytoplasmic RNA–interacting protein
202750_s_at	*TFIP11*	2.3	1.6E–3	Tuftelin-interacting protein 11
222748_s_at	*TXNL4B*	1.9	5.4E–4	Thioredoxin-like 4B
229630_s_at	*WTAP*	2.5	5.4E–4	Wilms tumor 1–associated protein
234295_at	*DBR1*	–1.7	7.9E–4	Debranching enzyme homolog 1 (*S cerevisiae*)
Ribosomal RNA processing				
201478_s_at	*DKC1*	1.8	1.0E–3	Dyskeratosis congenita 1, dyskerin
212422_at	*PDCD11*	1.6	4.1E–3	Programmed cell death 11

**Fold* denotes fold change between presurgical and postsurgical conditions.

TABLE E8. Expression of extracellular component genes in the diaphragm during cardiothoracic surgery

Probe set	Symbol	Fold*	*P* value	Description
Cell junction				
1553764_a_at	*JUB*	–1.8	1.4E–3	Jub, ajuba homolog (*Xenopus laevis*)
214212_x_at	*PLEKHC1*	1.7	1.1E–3	Pleckstrin homology domain containing, family C (with *FERM* domain) member 1
Extracellular matrix				
222162_s_at	*ADAMTS1*	4.1	1.5E–5	*ADAM* metallopeptidase with thrombospondin type 1 motif, 1
221541_at	*CRISPLD2*	2.8	2.8E–5	Cysteine-rich secretory protein LCCL domain containing 2
228190_at	*ATG4C*	–1.8	4.5E–3	ATG4 autophagy-related 4 homolog C (*Saccharomyces cerevisiae*)
201883_s_at	*B4GALT1*	1.9	2.7E–4	UDP-Gal:βGlcNAc β 1,4- galactosyltransferase, polypeptide 1
229900_at	*CD109*	2.0	2.4E–4	CD109 molecule
219522_at	*FJX1*	2.4	1.6E–3	Four-jointed box 1 (*Drosophila*)
238018_at	*hCG_1990170*	5.0	2.0E–7	Hypothetical protein LOC285016
205258_at	*INHBB*	4.3	2.2E–3	Inhibin, β B
226977_at	*LOC492311*	–1.6	3.9E–3	Similar to bovine IgA regulatory protein
225955_at	*LOC653506*	3.0	5.4E–5	Similar to meteorin, glial cell differentiation regulator–like
204575_s_at	*MMP19*	3.2	4.4E–3	Matrix metallopeptidase 19
206157_at	*PTX3*	20.5	9.0E–5	Pentraxin-related gene, rapidly induced by IL-1β
236953_s_at	*RP11-50D16.3*	–2.4	2.7E–3	Similar to *RIKEN* complementary DNA 8030451K01
236947_at	*SEMA3C*	–1.7	1.0E–3	Sema domain, immunoglobulin domain (Ig), short basic domain, secreted, (semaphorin) 3C
202376_at	*SERPINA3*	5.8	1.0E–5	Serpin peptidase inhibitor, clade A (α-1 antiproteinase, antitrypsin), member 3
201858_s_at	*SRGN*	4.2	1.2E–3	Serglycin
230746_s_at	*STC1*	7.6	3.1E–4	Stanniocalcin 1
241557_x_at	*TMEFF2*	1.7	3.9E–3	Transmembrane protein with endothelial growth factor–like and 2 follistatin-like domains 2
220975_s_at	*C1QTNF1*	2.0	1.6E–4	C1q and tumor necrosis factor–related protein 1
203592_s_at	*FSTL3*	1.6	1.2E–3	Follistatin-like 3 (secreted glycoprotein)
202638_s_at	*ICAM1*	3.4	1.4E–4	Intercellular adhesion molecule 1 (CD54), human rhinovirus receptor
210732_s_at	*LGALS8*	1.8	9.4E–4	Lectin, galactoside-binding, soluble, 8 (galectin 8)
Integral to membrane				
220948_s_at	*ATP1A1*	2.0	2.8E–4	Adenosine triphosphatase, Na^+/K^+ transporting, α 1 polypeptide
208836_at	*ATP1B3*	2.8	5.7E–5	Adenosine triphosphatase, Na^+/K^+ transporting, β 3 polypeptide
225612_s_at	*B3GNT5*	5.4	1.9E–5	UDP-GlcNAc:βGal β-1,3-N-acetylglucosaminyltransferase 5
221484_at	*B4GALT5*	1.9	6.3E–4	UDP-Gal:βGlcNAc β 1,4- galactosyltransferase, polypeptide 5
202710_at	*BET1*	–1.8	1.5E–3	*BET1* homolog (*S cerevisiae*)
227188_at	C21orf63	2.5	1.5E–4	Chromosome 21 open reading frame 63
202877_s_at	*CD93*	2.7	9.2E–4	CD93 molecule
203044_at	*CHSY1*	3.9	1.8E–5	Carbohydrate (chondroitin) synthase 1
202437_s_at	*CYP1B1*	1.9	3.8E–3	Cytochrome P-450, family 1, subfamily B, polypeptide 1
226402_at	*CYP2U1*	–1.6	4.7E–3	Cytochrome P-450, family 2, subfamily U, polypeptide 1
216513_at	*DCT*	3.0	3.1E–5	Dopachrome tautomerase (dopachrome δ-isomerase, tyrosine-related protein 2)
212856_at	*DIP*	1.6	3.4E–3	Death-inducing protein
230568_x_at	*DLL3*	1.6	2.6E–3	δ-like 3 (*Drosophila*)
238500_at	*EMP2*	1.5	4.1E–3	Epithelial membrane protein 2
232024_at	*GIMAP2*	–2.7	5.9E–4	Guanosine triphosphatase, *IMAP* family member 2
225424_at	*GPAM*	–2.1	1.7E–3	Glycerol-3-phosphate acyltransferase, mitochondrial
225222_at	*HIAT1*	1.7	1.4E–3	Hippocampus abundant transcript 1
227361_at	*HS3ST3B1*	2.0	1.2E–3	Heparan sulfate (glucosamine) 3-O-sulfotransferase 3B1
201631_s_at	*IER3*	3.6	8.6E–4	Immediate early response 3
201626_at	*INSIG1*	2.7	3.4E–3	Insulin-induced gene 1
206765_at	*KCNJ2*	–2.1	9.4E–4	Potassium inwardly rectifying channel, subfamily J, member 2
205303_at	*KCNJ8*	–1.7	4.3E–4	Potassium inwardly rectifying channel, subfamily J, member 8
202181_at	*KIAA0247*	1.8	6.2E–4	KIAA0247
205150_s_at	*KIAA0644*	–1.7	3.2E–3	*KIAA0644* gene product
239946_at	*KIAA0922*	–1.6	2.2E–3	KIAA0922
242762_s_at	*KIAA1946*	2.0	3.1E–4	KIAA1946
202068_s_at	*LDLR*	5.3	1.1E–6	Low-density lipoprotein receptor (familial hypercholesterolemia)
228762_at	*LFNG*	–2.0	7.0E–4	*LFNG* O-fucosylpeptide 3-beta-N-acetylglucosaminyltransferase

(Continued)

TABLE E8. Continued

Probe set	Symbol	Fold*	*P* value	Description
222231_s_at	*LRRC59*	2.0	1.0E–3	Leucine-rich repeat containing 59
224624_at	*LRRC8A*	1.8	3.2E–3	Leucine-rich repeat containing 8 family, member A
219003_s_at	*MANEA*	–1.5	2.9E–3	Mannosidase, endo-α
229531_at	*MCART6*	–1.5	2.8E–3	Mitochondrial carrier triple repeat 6
228282_at	*MFSD8*	–1.7	4.4E–3	Major facilitator superfamily domain containing 8
1569136_at	*MGAT4A*	2.3	7.1E–4	Mannosyl (α-1,3-)-glycoprotein β-1,4-N-acetylglucosaminyltransferase, isozyme A
203780_at	*MPZL2*	2.3	1.6E–3	Myelin protein zero–like 2
223276_at	*MST150*	2.7	2.7E–4	MSTP150
224920_x_at	*MYADM*	1.7	3.5E–3	Myeloid-associated differentiation marker
1564746_at	*NHEDC2*	1.5	4.6E–3	Na^+/H^+ exchanger domain containing 2
225975_at	*PCDH18*	–2.3	6.1E–4	Protocadherin 18
205077_s_at	*PIGF*	–1.5	3.4E–3	Phosphatidylinositol glycan anchor biosynthesis, class F
51146_at	*PIGV*	–1.8	4.2E–3	Phosphatidylinositol glycan anchor biosynthesis, class V
202446_s_at	*PLSCR1*	3.3	6.3E–5	Phospholipid scramblase 1
1569641_at	*PQLC1*	1.5	2.6E–3	PQ loop repeat containing 1
226021_at	*RDH10*	2.8	1.4E–4	Retinol dehydrogenase 10 (all trans)
219897_at	*RNF122*	1.6	3.1E–3	Ring finger protein 122
226104_at	*RNF170*	–1.7	3.4E–3	Ring finger protein 170
229199_at	*SCN9A*	–1.8	3.4E–3	Sodium channel, voltage-gated, type IX, alpha subunit
206211_at	*SELE*	6.0	3.5E–5	Selectin E (endothelial adhesion molecule 1)
205856_at	*SLC14A1*	–2.4	6.5E–4	Solute carrier family 14 (urea transporter), member 1 (Kidd blood group)
209681_at	*SLC19A2*	3.3	5.9E–5	Solute carrier family 19 (thiamine transporter), member 2
205896_at	*SLC22A4*	3.6	2.3E–5	Solute carrier family 22 (organic cation transporter), member 4
221662_s_at	*SLC22A7*	1.7	9.0E–4	Solute carrier family 22 (organic anion transporter), member 7
225212_at	*SLC25A25*	3.8	1.3E–5	Solute carrier family 25 (mitochondrial carrier; phosphate carrier), member 25
221020_s_at	*SLC25A32*	1.8	1.8E–3	Solute carrier family 25, member 32
32091_at	*SLC25A44*	1.7	1.5E–3	Solute carrier family 25, member 44
222088_s_at	*SLC2A14*	3.9	4.2E–6	Solute carrier family 2 (facilitated glucose transporter), member 14
223044_at	*SLC40A1*	–1.7	1.5E–3	Solute carrier family 40 (iron-regulated transporter), member 1
219911_s_at	*SLCO4A1*	3.0	6.2E–5	Solute carrier organic anion transporter family, member 4A1
221561_at	*SOAT1*	2.0	3.6E–3	Sterol O-acyltransferase (acylcoenzyme A: cholesterol acyltransferase) 1
212470_at	*SPAG9*	1.5	2.9E–3	Sperm-associated antigen 9
203127_s_at	*SPTLC2*	1.7	4.5E–3	Serine palmitoyltransferase, long chain base subunit 2
212112_s_at	*STX12*	1.7	9.6E–4	Syntaxin 12
226489_at	*TMCC3*	1.7	1.2E–3	Transmembrane and coiled-coil domain family 3
226825_s_at	*TMEM165*	2.0	2.2E–4	Transmembrane protein 165
219253_at	*TMEM185B*	1.6	8.8E–4	Transmembrane protein 185B
218113_at	*TMEM2*	3.3	7.5E–5	Transmembrane protein 2
231697_s_at	*TMEM49*	2.3	3.5E–3	Transmembrane protein 49
1557520_a_at	*TMEM59*	1.5	3.4E–3	Transmembrane protein 59
219449_s_at	*TMEM70*	1.5	3.4E–3	Transmembrane protein 70
223772_s_at	*TMEM87A*	1.8	3.3E–3	Transmembrane protein 87A
204881_s_at	*UGCG*	5.0	5.1E–6	UDP-glucose ceramide glucosyltransferase
224953_at	*YIPF5*	–1.6	4.2E–3	Yip1 domain family, member 5
222451_s_at	*ZDHHC9*	2.2	1.7E–3	Zinc finger, DHHC-type containing 9
209186_at	*ATP2A2*	1.9	8.3E–4	Adenosine triphosphatase, Ca^{2+} transporting, cardiac muscle, slow twitch 2
202669_s_at	*EFNB2*	1.6	1.7E–3	Ephrin-B2
204359_at	*FLRT2*	–2.1	4.0E–4	Fibronectin leucine-rich transmembrane protein 2
222853_at	*FLRT3*	–2.6	2.8E–3	Fibronectin leucine rich transmembrane protein 3
207316_at	*HAS1*	3.8	6.0E–5	Hyaluronan synthase 1
206432_at	*HAS2*	4.5	3.4E–5	Hyaluronan synthase 2
213620_s_at	*ICAM2*	1.8	7.2E–4	Intercellular adhesion molecule 2
203835_at	*LRRC32*	2.0	1.3E–4	Leucine-rich repeat containing 32
230494_at	*SLC20A1*	2.6	7.6E–6	Solute carrier family 20 (phosphate transporter), member 1
243166_at	*SLC30A5*	–1.5	2.9E–3	Solute carrier family 30 (zinc transporter), member 5

(Continued)

TABLE E8. Continued

Probe set	Symbol	Fold*	*P* value	Description
209387_s_at	*TM4SF1*	2.3	4.1E–3	Transmembrane 4 L six family member 1
Plasma membrane				
209122_at	*ADFP*	1.9	3.3E–3	Adipose differentiation–related protein
227439_at	*ANKS1B*	1.8	3.9E–3	Ankyrin repeat and sterile alpha motif domain containing 1B
208536_s_at	*BCL2L11*	1.5	3.7E–3	BCL2-like 11 (apoptosis facilitator)
204995_at	*CDK5R1*	1.6	3.0E–3	Cyclin-dependent kinase 5, regulatory subunit 1 (p35)
217291_at	*CEACAM5*	1.5	3.0E–3	Carcinoembryonic antigen–related cell adhesion molecule 5
219492_at	*CHIC2*	1.8	2.1E–3	Cysteine-rich hydrophobic domain 2
1559258_a_at	CXorf61	1.6	4.4E–3	Chromosome X open reading frame 61
212515_s_at	*DDX3X*	1.8	8.5E–4	*DEAD* (Asp-Glu-Ala-Asp) box polypeptide 3, X-linked
205000_at	*DDX3Y*	2.0	3.3E–4	*DEAD* (Asp-Glu-Ala-Asp) box polypeptide 3, Y-linked
1558511_s_at	*FAM62B*	1.6	2.0E–3	Family with sequence similarity 62 (C2 domain containing) member B
225582_at	*KIAA1754*	3.7	3.8E–5	KIAA1754
212086_x_at	*LMNA*	1.9	4.5E–3	Lamin A/C
202760_s_at	*PALM2-AKAP2*	2.1	2.8E-03	PALM2-AKAP2 protein
204715_at	*PANX1*	1.9	3.9E–3	Pannexin 1
214827_at	*PARD6B*	1.8	3.7E–4	Par-6 partitioning defective 6 homolog β (*Caenorhabditis elegans*)
209355_s_at	*PPAP2B*	2.1	9.4E–4	Phosphatidic acid phosphatase type 2B
226430_at	*RELL1*	1.6	3.0E–3	RELT-like 1
241771_at	*RIMBP2*	1.9	3.8E–3	RIMS binding protein 2
201739_at	*SGK*	2.2	1.1E–3	Serum/glucocorticoid-regulated kinase
212110_at	*SLC39A14*	4.1	1.2E–4	Solute carrier family 39 (zinc transporter), member 14
221752_at	*SSH1*	1.5	3.0E–3	Slingshot homolog 1 (*Drosophila*)
225987_at	*STEAP4*	1.9	1.8E–3	*STEAP* family member 4
201060_x_at	*STOM*	2.3	3.4E–4	Stomatin
235670_at	*STX11*	2.5	1.7E–4	Syntaxin 11
237252_at	*THBD*	6.7	1.5E–5	Thrombomodulin
202085_at	*TJP2*	1.8	2.0E–4	Tight junction protein 2 (zona occludens 2)
231853_at	*TUBD1*	–1.6	2.4E–3	Tubulin, δ 1
Proteinaceous extracellular matrix				
210809_s_at	*POSTN*	1.8	4.9E–3	Periostin, osteoblast specific factor
37022_at	*PRELP*	1.6	3.2E–3	Proline/arginine-rich end leucine-rich repeat protein

**Fold* denotes fold change between presurgical and postsurgical conditions.

TABLE E9. Expression of transporter activity genes in the diaphragm during cardiothoracic surgery

Probe set	Symbol	Fold*	P value	Description
Carbohydrate transport				
200787_s_at	*PEA15*	1.8	6.8E–4	Phosphoprotein enriched in astrocytes 15
Electron transport chain				
241755_at	*UQCRC2*	–1.7	3.2E–3	Ibiquinol–cytochrome c reductase core protein II
Endoplasmic reticulum to Golgi vesicle–mediated transport				
212902_at	*SEC24A*	1.8	1.2E–3	*SEC24*-related gene family, member A (*Saccharomyces cerevisiae*)
Glucose transport				
202932_at	*YES1*	1.7	1.1E–3	*v-yes-1* Yamaguchi sarcoma viral oncogene homolog 1
Glycolipid transport				
227247_at	*PLEKHA8*	–1.5	2.2E–3	Pleckstrin homology domain containing, family A (phosphoinositide-binding specific) member 8
Intracellular protein transmembrane transport				
241425_at	*NUPL1*	1.4	4.6E–3	Nucleoporin-like 1
223225_s_at	*SEH1L*	2.6	2.1E–3	SEH1-like (*S cerevisiae*)
Intracellular protein transport				
207624_s_at	*RPGR*	1.7	9.7E–4	Retinitis pigmentosa guanosine triphosphatase regulator
Metal ion transport				
237648_x_at	*NHEDC2*	1.6	1.9E–3	Na^+/H^+ exchanger domain containing 2
243524_at	*SLC30A7*	2.0	5.9E–4	Solute carrier family 30 (zinc transporter), member 7
1561886_a_at	*SLC39A14*	3.4	3.2E–6	Solute carrier family 39 (zinc transporter), member 14
Neurotransmitter transport				
1569916_at	*SLC6A15*	2.1	6.6E–4	Solute carrier family 6, member 15
Potassium ion transport				
230192_at	*TRIM13*	–1.5	8.8E–4	Tripartite motif-containing 13
Protein transport				
229953_x_at	*LCA5*	–1.9	3.2E–3	Leber congenital amaurosis 5
218708_at	*NXT1*	2.6	1.8E–4	NTF2-like export factor 1
221704_s_at	*VPS37B*	1.5	3.5E–3	Vacuolar protein sorting 37 homolog B (*S cerevisiae*)
211762_s_at	*KPNA2*	2.4	1.3E–3	Karyopherin α 2 (RAG cohort 1, importin α 1)
Retrograde axon cargo transport				
208093_s_at	*NDEL1*	1.9	1.1E–4	nudE nuclear distribution gene E homolog (*Aspergillus nidulans*)–like 1
Transporter activity				
212168_at	*RBM12*	1.6	2.5E–3	RNA-binding motif protein 12

**Fold* denotes fold change between presurgical and postsurgical conditions.

TABLE E10. Expression of binding genes in the diaphragm during cardiothoracic surgery

Probe set	Symbol	Fold*	*P* value	Description
Antigen binding				
202886_s_at	*PPP2R1B*	1.7	1.7E–3	Protein phosphatase 2 (formerly 2A), regulatory subunit A, β isoform
Adenosine triphosphate binding				
230387_at	*ATP2C1*	–1.6	3.1E–3	Adenosine triphosphatase, Ca^{2+} transporting, type 2C, member 1
224454_at	*ETNK1*	4.0	5.3E–5	Ethanolamine kinase 1
221918_at	*PCTK2*	1.9	4.3E–4	PCTAIRE protein kinase 2
227255_at	*PDIK1L*	–1.6	1.5E–3	PDLIM1 interacting kinase 1 like
1568768_s_at	*RBKS*	6.7	5.5E–5	Ribokinase
236114_at	*RUNX1*	2.7	3.3E–4	Runt-related transcription factor 1 (acute myeloid leukemia 1; aml1 oncogene)
205214_at	*STK17B*	3.3	2.0E–3	Serine/threonine kinase 17b
Binding				
1555281_x_at	*ARMC8*	1.7	2.0E–3	Armadillo repeat containing 8
221003_s_at	*CAB39L*	2.0	3.1E–4	Calcium binding protein 39–like
230289_at	*EPB41L1*	2.4	3.9E–3	Erythrocyte membrane protein band 4.1–like 1
226038_at	*LONRF1*	1.6	3.7E–4	LON peptidase N-terminal domain and ring finger 1
201761_at	*MTHFD2*	2.4	2.0E–4	methylenetetrahydrofolate dehydrogenase (nicotinamide adenine dinucleotide phosphate^{+}–dependent) 2, methylenetetrahydrofolate cyclohydrolase
202083_s_at	*SEC14L1*	2.4	1.4E–4	SEC14-like 1 (*Saccharomyces cerevisiae*)
229169_at	*TTC18*	–1.5	4.8E–3	Tetratricopeptide repeat domain 18
1554588_a_at	*TTC30B*	–2.0	1.0E–4	Tetratricopeptide repeat domain 30B
Calcium ion binding				
225656_at	*EFHC1*	1.9	2.4E–4	EF-hand domain (C-terminal) containing 1
Carbohydrate binding				
224826_at	*RP5–1022P6.2*	1.7	1.7E–3	Hypothetical protein KIAA1434
DNA binding				
220936_s_at	*H2AFJ*	–1.7	2.5E–3	H2A histone family, member J
205436_s_at	*H2AFX*	1.8	3.5E–3	H2A histone family, member X
211997_x_at	*H3F3B*	1.9	9.8E–5	H3 histone, family 3B (H3.3B)
232035_at	*HIST1H4H*	2.2	1.8E–3	Histone cluster 1, H4h
222139_at	*KIAA1466*	1.7	4.1E–3	*KIAA1466* gene
1557852_at	*PHC2*	2.2	6.4E–4	Polyhomeotic homolog 2 (*Drosophila*)
217741_s_at	*ZFAND5*	3.9	3.8E–5	Zinc finger, AN1-type domain 5
Drug binding				
203302_at	*DCK*	–1.7	2.0E–3	Deoxycytidine kinase
Guanosine triphosphate binding				
205140_at	*FPGT*	–1.7	1.0E–3	Fucose-1-phosphate guanylyltransferase
209191_at	*TUBB6*	3.0	1.9E–4	Tubulin, β 6
Identical protein binding				
200648_s_at	*GLUL*	2.1	1.2E–3	Glutamate-ammonia ligase (glutamine synthetase)
Iron-sulfur cluster binding				
201873_s_at	*ABCE1*	1.5	5.0E–3	Adenosine triphosphate–binding cassette, subfamily E (OABP), member 1
Lipid binding				
235985_at	*PITPNB*	1.9	8.2E–4	Phosphatidylinositol transfer protein, β
Magnesium ion binding				
225613_at	*MAST4*	1.9	4.0E–3	Microtubule-associated serine/threonine kinase family member 4
206177_s_at	*ARG1*	4.5	3.8E–3	Arginase, liver
210005_at	*GART*	1.7	1.3E–3	Phosphoribosylglycinamide formyltransferase, phosphoribosylglycinamide synthetase, phosphoribosylaminoimidazole synthetase
Metal ion binding				
1559391_s_at	*B4GALT5*	2.2	1.9E–4	UDP-Gal:βGlcNAc β 1,4- galactosyltransferase, polypeptide 5
200768_s_at	*MAT2A*	2.5	1.2E–4	methionine adenosyltransferase II, α
236699_at	*MBNL2*	1.4	3.9E–3	Muscleblind-like 2 (*Drosophila*)
241583_x_at	*SYT1*	1.7	1.2E–3	Synaptotagmin I
212665_at	*TIPARP*	6.2	4.0E–7	*TCDD*-inducible poly(adenosine diphosphate–ribose) polymerase

(Continued)

TABLE E10. Continued

Probe set	Symbol	Fold*	*P* value	Description
218810_at	*ZC3H12A*	2.1	5.9E–4	Zinc finger CCCH-type containing 12A
201531_at	*ZFP36*	4.5	2.2E–6	Zinc finger protein 36, C3H type, homolog (mouse)
Nucleic acid binding				
220359_s_at	*ARPP-21*	6.0	2.4E–4	Cyclic adenosine monophosphate–regulated phosphoprotein, 21 kDa
241858_at	*FPGT*	–2.0	2.7E–3	Fucose-1-phosphate guanylyltransferase
224632_at	*GPATCH4*	1.6	1.2E–3	G patch domain containing 4
238829_at	*SPG11*	1.5	3.2E–3	Spastic paraplegia 11 (autosomal recessive)
230380_at	*THAP2*	3.4	9.2E–4	*THAP* domain containing, apoptosis-associated protein 2
228201_at	*ARL13B*	1.7	9.2E–4	adenosine diphosphate ribosylation factor–like 13B
219487_at	*BBS10*	–1.9	4.4E–3	Bardet–Biedl syndrome 10
208896_at	*DDX18*	1.6	2.3E–3	*DEAD* (Asp-Glu-Ala-Asp) box polypeptide 18
208152_s_at	*DDX21*	3.1	4.6E–4	*DEAD* (Asp-Glu-Ala-Asp) box polypeptide 21
1568815_a_at	*DDX50*	1.7	8.0E–4	*DEAD* (Asp-Glu-Ala-Asp) box polypeptide 50
219243_at	*GIMAP4*	–1.7	3.0E–3	Guonosine triphosphatase, *IMAP* family member 4
228071_at	GIMAP7	–2.0	6.5E–4	Guanosine triphosphatase, *IMAP* family member 7
240452_at	*GSPT1*	2.1	4.2E–5	G1 to S phase transition 1
213076_at	*ITPKC*	3.7	4.7E–6	Inositol 1,4,5-trisphosphate 3-kinase C
223380_s_at	*LATS2*	1.6	4.2E–3	LATS, large tumor suppressor, homolog 2 (*Drosophila*)
238122_at	*RBM12B*	–1.8	2.1E–4	RNA binding motif protein 12B
202693_s_at	*STK17A*	2.0	2.7E–3	Serine/threonine kinase 17a
Phosphoinositide binding				
212923_s_at	C6orf145	3.1	1.9E–5	Chromosome 6 open reading frame 145
220330_s_at	*SAMSN1*	6.7	1.0E–3	*SAM* domain, *SH3* domain, and nuclear localization signals 1
Protein binding				
218723_s_at	C13orf15	2.6	2.3E–4	Chromosome 13 open reading frame 15
230424_at	C5orf13	–1.7	1.7E–3	Chromosome 5 open reading frame 13
236634_at	C8orf48	–1.6	3.5E–3	Chromosome 8 open reading frame 48
205899_at	*CCNA1*	1.5	3.2E–3	Cyclin A1
218351_at	*COMMD8*	–1.6	3.3E–3	*COMM* domain containing 8
208892_s_at	*DUSP6*	2.5	2.4E–3	Dual specificity phosphatase 6
220386_s_at	*EML4*	1.7	6.2E–4	Echinoderm microtubule-associated protein–like 4
224657_at	*ERRFI1*	4.0	1.2E–6	ERBB receptor feedback inhibitor 1
214509_at	*HIST1H3I*	1.6	2.8E–3	Histone cluster 1, H3i
225142_at	*JHDM1D*	1.6	3.3E–3	Jumonji C domain-containing histone demethylase 1 homolog D (*S cerevisiae*)
226479_at	*KBTBD6*	–1.8	2.5E–3	Kelch repeat and BTB (POZ) domain containing 6
223412_at	*KBTBD7*	–2.0	2.4E–4	Kelch repeat and BTB (POZ) domain containing 7
243589_at	*KIAA1267*	–1.6	3.2E–3	KIAA1267
226370_at	*KLHL15*	1.7	3.7E–3	Kelch-like 15 (*Drosophila*)
203068_at	*KLHL21*	1.6	2.8E–3	Kelch-like 21 (*Drosophila*)
1559580_at	*LRRC39*	–3.1	6.0E–4	Leucine-rich repeat containing 39
200712_s_at	*MAPRE1*	1.4	3.5E–3	Microtubule-associated protein, RP/EB family, member 1
225478_at	*MFHAS1*	1.9	2.3E–4	Malignant fibrous histiocytoma amplified sequence 1
223397_s_at	*NIP7*	2.7	8.3E–4	Nuclear import 7 homolog (*S cerevisiae*)
1555310_a_at	*PAK6*	1.7	8.1E–4	p21 (CDKN1A)–activated kinase 6
211564_s_at	*PDLIM4*	1.8	2.2E–3	PDZ and *LIM* domain 4
202464_s_at	*PFKFB3*	3.8	1.4E–4	6-Phosphofructo-2-kinase/fructose-2,6-biphosphatase 3
200919_at	*PHC2*	2.0	2.5E–3	Polyhomeotic homolog 2 (*Drosophila*)
217996_at	*PHLDA1*	3.8	7.9E–4	Pleckstrin homology–like domain, family A, member 1
209317_at	*POLR1C*	1.9	1.3E–3	Polymerase (RNA) I polypeptide C, 30 kDa
37028_at	*PPP1R15A*	2.2	1.7E–3	Protein phosphatase 1, regulatory (inhibitor) subunit 15A
205178_s_at	*RBBP6*	1.8	2.0E–4	Retinoblastoma binding protein 6
225039_at	*RPE*	–1.5	2.5E–3	Ribulose-5-phosphate-3-epimerase
209486_at	SAS10	2.0	1.2E–3	Disrupter of silencing 10
236606_at	SAV1	1.5	1.2E–3	Salvador homolog 1 (*Drosophila*)
226337_at	SCYL1BP1	–1.9	2.1E–3	SCY1-like 1 binding protein 1

(Continued)

TABLE E10. Continued

Probe set	Symbol	Fold*	*P* value	Description
219480_at	*SNAI1*	1.6	3.0E–3	Snail homolog 1 (*Drosophila*)
218335_x_at	*TNIP2*	1.6	4.3E–3	TNFAIP3 interacting protein 2
235081_x_at	*TRIM65*	–1.7	8.6E–4	Tripartite motif-containing 65
233970_s_at	*TRMT6*	1.6	1.1E–3	Transfer RNA methyltransferase 6 homolog (*S cerevisiae*)
218156_s_at	*TSR1*	1.6	1.5E–3	TSR1, 20S ribonuclear RNA accumulation, homolog (*S cerevisiae*)
209251_x_at	*TUBA1C*	1.5	2.4E–3	Tubulin, α 1c
218647_s_at	*YRDC*	2.0	2.3E–4	yrdC domain containing (*E coli*)
218214_at	C12orf44	1.5	1.5E–3	Chromosome 12 open reading frame 44
211947_s_at	*BAT2D1*	1.5	2.7E–3	*BAT2* domain containing 1
213918_s_at	*NIPBL*	1.7	2.0E–4	Nipped-B homolog (*Drosophila*)
218738_s_at	*RNF138*	1.8	2.7E–3	Ring finger protein 138
Rab guanosine triphosphatase binding				
222333_at	*ALS2CL*	1.9	4.6E–4	ALS2 C-terminal like
RNA binding				
224956_at	*NUFIP2*	1.8	4.8E–3	Nuclear fragile X mental retardation protein interacting protein 2
236907_at	*PABPC1*	2.2	9.7E–4	Poly(A) binding protein, cytoplasmic 1
220104_at	*ZC3HAV1*	2.1	4.0E–4	Zinc finger CCCH-type, antiviral 1
201369_s_at	*ZFP36L2*	2.2	2.2E–5	Zinc finger protein 36, C3H type–like 2
201530_x_at	*EIF4A1*	2.6	4.5E–4	Eukaryotic translation initiation factor 4A, isoform 1
Single-stranded DNA binding				
233085_s_at	*OBFC2A*	2.7	5.4E–4	Oligonucleotide/oligosaccharide-binding fold containing 2A
Spermidine binding				
213988_s_at	*SAT1*	2.8	2.8E–4	Spermidine/spermine N1-acetyltransferase 1
Unfolded protein binding				
208977_x_at	*TUBB2C*	1.6	3.3E–3	Tubulin, β 2C
Zinc ion binding				
231270_at	*CA13*	1.7	3.7E–3	Carbonic anhydrase XIII
223800_s_at	*LIMS3*	2.4	5.1E–5	LIM and senescent cell antigen–like domains 3
202643_s_at	*TNFAIP3*	3.2	2.1E–3	Tumor necrosis factor α–induced protein 3
211965_at	*ZFP36L1*	3.0	4.5E–5	Zinc finger protein 36, C3H type–like 1

**Fold* denotes fold change between presurgical and postsurgical conditions.

TABLE E11. Expression of miscellaneous and unknown genes in the diaphragm during cardiothoracic surgery

Probe set	Symbol	Fold*	*P* value	Description	Function
226621_at	*FGG*	3.0	3.9E–5	Fibrinogen γ chain	Associates with IL31RA to form the interleukin 31 receptor
242836_at	*ATP1B3*	2.6	4.2E–4	Adenosine triphosphatase, Na^+/K^+ transporting, β 3 polypeptide	Adenosine triphosphate metabolism
241916_at	*PLSCR1*	1.8	6.3E–4	Phospholipid scramblase 1	Blood coagulation
242868_at	*EPAS1*	2.2	3.0E–5	Endothelial *PAS* domain protein 1	Blood vessel development
240815_at	*SEMA3C*	–1.7	2.9E–3	Sema domain, immunoglobulin domain (Ig), short basic domain, secreted, (semaphorin) 3C	Blood vessel development
231999_at	*ANKRD11*	1.5	4.3E–3	Ankyrin repeat domain 11	Bone development
209585_s_at	*MINPP1*	–1.6	3.8E–3	Multiple inositol polyphosphate histidine phosphatase, 1	Bone development
1562275_at	*ADAMTS9*	8.4	7.4E–5	ADAM metallopeptidase with thrombospondin type 1 motif, 9	Cleaves the large aggregating proteoglycans, aggrecan and versican
225699_at	*SNORA9*	2.5	5.7E–5	Small nucleolar RNA, H/ACA box 9	Core component of the SMC5-SMC6 complex, a complex involved in DNA double-strand breaks by homologous recombination
1562948_at	*SMC5*	1.5	4.1E–3	Structural maintenance of chromosomes 5	DNA metabolic process
242116_x_at	*ANKRD17*	1.6	2.6E–3	Ankyrin repeat domain 17	Earliest specific in situ marker of hepatic differentiation during embryogenesis
218361_at	*GOLPH3L*	–1.9	2.2E–3	Golgi phosphoprotein 3–like	Golgi apparatus
225912_at	*TP53INP1*	–1.9	4.8E–3	Tumor protein p53 inducible nuclear protein 1	In response to double-strand DNA breaks, promotes p53/TP53 phosphorylation on Ser-46 and subsequent apoptosis
228772_at	*HNMT*	–1.8	4.4E–3	Histamine N-methyltransferase	Inactivates histamine by N-methylation; plays an important role in degrading histamine and in regulating airway response to histamine
1565638_at	*PMP22*	1.6	4.9E–3	Peripheral myelin protein 22	Involved in growth regulation and in myelinization in the peripheral nervous system
234639_x_at	*KRTAP9-8*	–1.7	3.6E–3	Keratin-associated protein 9–8	Keratin filament
201196_s_at	*AMD1*	2.3	1.1E–3	Adenosylmethionine decarboxylase 1	Lyase activity
214911_s_at	*BRD2*	1.7	4.1E–3	Bromodomain containing 2	May play a role in spermatogenesis or folliculogenesis
237007_at	*KCNB2*	1.6	8.3E–4	Potassium voltage-gated channel, Shab-related subfamily, member 2	Mediates the voltage-dependent potassium ion permeability of excitable membranes
230333_at	*SAT1*	1.8	4.1E–3	Spermidine/spermine N1-acetyltransferase 1	N-acyltransferase activity
222142_at	*CYLD*	1.4	3.3E–3	Cylindromatosis (turban tumor syndrome)	Negative regulator of *TRAF2* and neutral factor κB signaling pathway
202238_s_at	*NNMT*	4.0	1.0E–5	Nicotinamide N-methyltransferase	N-methyltransferase activity
203023_at	*HSPC111*	1.9	5.4E–4	Hypothetical protein HSPC111	Nuclear lumen
211686_s_at	*RBM13*	1.7	3.6E–3	RNA-binding motif protein 13	Nuclear lumen
203234_at	*UPP1*	3.2	1.0E–4	Uridine phosphorylase 1	Nucleobase, nucleoside, nucleotide, and nucleic acid metabolic process
238902_at	*PCMTD1*	–1.5	2.0E–3	Protein-L-isoaspartate (D-aspartate) O-methyltransferase domain containing 1	O-methyltransferase activity
209457_at	*DUSP5*	2.5	2.8E–5	Dual specificity phosphatase 5	Phosphatase activity
239516_at	*LYPLAL1*	–3.5	2.3E–4	Lysophospholipase-like 1	Phosphatase activity
209803_s_at	*PHLDA2*	3.5	1.2E–5	Pleckstrin homology–like domain, family A, member 2	Plays a role in regulating placenta growth
219677_at	*SPSB1*	2.3	7.8E–5	splA/ryanodine receptor domain and *SOCS* box containing 1	Substrate recognition component of SCF-like ECS complex
223580_at	*SPSB2*	–1.5	2.6E–3	splA/ryanodine receptor domain and *SOCS* box containing 2	Substrate recognition component of SCF-like ECS complex

(Continued)

TABLE E11. Continued

Probe set	Symbol	Fold*	*P* value	Description	Function
204014_at	*DUSP4*	1.8	4.7E–3	Dual specificity phosphatase 4	Regulates mitogenic signal transduction by dephosphorylating both Thr and Tyr residues on MAP kinases ERK1 and ERK2
227621_at	*WTAP*	2.5	3.3E–3	Wilms tumor 1 associated protein	RNA splicing
215095_at	*ESD*	–1.5	3.7E–3	Esterase D/formylglutathione hydrolase	Serine hydrolase involved in the detoxification of formaldehyde
235419_at	*ERRFI1*	2.1	6.9E–5	ERBB receptor feedback inhibitor 1	Small guanosine triphosphatase regulator activity
203276_at	*LMNB1*	4.0	5.0E–4	Lamin B1	Structural molecular activity
225735_at	*ANKRD50*	–1.5	3.4E–3	Ankyrin repeat domain 50	Unknown
226055_at	ARRDC2	1.7	7.6E–4	Arrestin domain containing 2	Unknown
229437_at	*BIC*	2.7	8.4E–4	BIC transcript	Unknown
226383_at	C11orf46	–1.7	3.2E–3	Chromosome 11 open reading frame 46	Unknown
227058_at	C13orf33	4.0	1.4E–4	Chromosome 13 open reading frame 33	Unknown
227446_s_at	C14orf167	–1.9	3.3E–3	Chromosome 14 open reading frame 167	Unknown
212643_at	C14orf32	1.4	3.6E–3	Chromosome 14 open reading frame 32	Unknown
223474_at	C14orf4	1.6	3.9E–3	Chromosome 14 open reading frame 4	Unknown
217682_at	C16orf72	1.9	3.7E–4	Chromosome 16 open reading frame 72	Unknown
213528_at	C1orf156	–1.8	6.2E–4	Chromosome 1 open reading frame 156	Unknown
244103_at	C1orf55	1.7	1.9E–3	Chromosome 1 open reading frame 55	Unknown
209020_at	C20orf111	1.7	3.0E–3	Chromosome 20 open reading frame 111	Unknown
241484_x_at	C20orf80	–1.5	2.9E–3	Chromosome 20 open reading frame 80	Unknown
1552605_s_at	C21orf74	1.5	2.3E–3	Chromosome 21 open reading frame 74	Unknown
228067_at	C2orf55	2.4	8.4E–4	Chromosome 2 open reading frame 55	Unknown
222309_at	C6orf62	2.4	3.0E–3	Chromosome 6 open reading frame 62	Unknown
222706_at	*CCDC49*	1.5	3.7E–3	Coiled-coil domain containing 49	Unknown
1553214_a_at	*CCDC7*	–1.7	2.7E–3	Coiled-coil domain containing 7	Unknown
227517_s_at	*CENPL*	2.0	6.7E–4	Centromere protein L	Unknown
229718_at	*CG018*	1.9	1.9E–3	Hypothetical gene CG018	Unknown
224991_at	*CMIP*	1.9	4.7E–3	c-Maf–inducing protein	Unknown
1563536_at	*COL4A5*	1.5	1.4E–3	Collagen, type IV, α 5 (Alport syndrome)	Unknown
219397_at	*COQ10B*	1.9	3.4E–4	Coenzyme Q10 homolog B (*Saccharomyces cerevisiae*)	Unknown
1563445_x_at	*CTSLL3*	2.5	1.5E–5	Cathepsin L–like 3	Unknown
227520_at	CXorf15	1.6	4.6E–3	Chromosome X open reading frame 15	Unknown
1556114_a_at	*DKFZp451A211*	3.2	2.3E–4	DKFZp451A211 protein	Unknown
1569987_at	*DLEU7*	–1.5	4.5E–3	Deleted in lymphocytic leukemia, 7	Unknown
236649_at	*DTWD1*	–1.8	9.5E–4	*DTW* domain containing 1	Unknown
1563315_s_at	*ERICH1*	1.8	9.3E–4	Glutamate-rich 1	Unknown
219216_at	*ETAA1*	–2.0	1.2E–3	Ewing tumor–associated antigen 1	Unknown
223038_s_at	*FAM60A*	1.7	3.7E–3	Family with sequence similarity 60, member A	Unknown
244014_x_at	*FAM92A1*	–1.6	3.8E–3	Family with sequence similarity 92, member A1	Unknown
1553797_a_at	*FLJ30594*	–2.3	4.4E–3	Hypothetical locus FLJ30594	Unknown
229521_at	*FLJ36031*	4.8	8.0E–7	Hypothetical protein FLJ36031	Unknown
239331_at	*FLJ43663*	2.7	1.1E–4	Hypothetical protein FLJ43663	Unknown
236583_at	*GIMAP5*	–1.7	2.3E–3	Guanosine triphosphatase, *IMAP* family member 5	Unknown
233599_at	*hCG_2003663*	–1.7	8.3E–4	hCG2003663	Unknown
202081_at	*IER2*	2.9	1.8E–3	Immediate early response 2	Unknown
218611_at	*IER5*	2.6	1.3E–3	Immediate early response 5	Unknown
203143_s_at	*KIAA0040*	4.2	6.6E–6	KIAA0040	Unknown
228325_at	*KIAA0146*	5.6	2.0E–7	KIAA0146	Unknown
225924_at	*KIAA1450*	1.8	1.5E–3	KIAA1450 protein	Unknown
228334_x_at	*KIAA1712*	–1.6	2.7E–3	KIAA1712	Unknown
231828_at	*LOC253039*	–2.1	3.0E–3	Hypothetical protein LOC253039	Unknown
235151_at	*LOC283357*	–1.6	3.5E–3	Hypothetical protein LOC283357	Unknown
229007_at	*LOC283788*	–1.7	4.1E–3	Hypothetical protein LOC283788	Unknown

(Continued)

TABLE E11. Continued

Probe set	Symbol	Fold*	*P* value	Description	Function
234141_s_at	*LOC286059*	1.8	2.5E–3	Hypothetical protein LOC286059	Unknown
227099_s_at	*LOC387763*	3.8	1.7E–4	Hypothetical LOC387763	Unknown
225857_s_at	*LOC388796*	1.8	8.1E–4	Hypothetical LOC388796	Unknown
228603_at	*LOC440900*	1.5	2.2E–3	Hypothetical LOC440900	Unknown
230595_at	*LOC572558*	–1.5	2.9E–3	Hypothetical locus LOC572558	Unknown
220770_s_at	*LOC63920*	–2.3	2.2E–4	Transposon-derived Buster3 transposase-like	Unknown
203742_s_at	*LOC645233*	1.5	4.5E–3	Similar to G/T mismatch–specific thymine DNA glycosylase	Unknown
240421_x_at	*LOC646561*	1.8	2.7E–3	Similar to WW45 protein	Unknown
239343_at	*LOC728705*	–1.4	3.3E–3	Hypothetical protein LOC728705	Unknown
1556180_at	*LOC729678*	–1.6	4.1E–3	Hypothetical protein LOC729678	Unknown
215322_at	*LONRF1*	1.8	2.9E–3	LON peptidase N-terminal domain and ring finger 1	Unknown
224558_s_at	*MALAT1*	1.4	4.2E–3	Metastasis-associated lung adenocarcinoma transcript 1 (noncoding RNA)	Unknown
213761_at	*MDM1*	–1.6	3.1E–3	Mdm4, transformed 3T3 cell double minute 1, p53 binding protein (mouse)	Unknown
214696_at	*MGC14376*	2.5	4.0E–4	Hypothetical protein MGC14376	Unknown
236273_at	*NBPF1*	–1.4	4.7E–3	Neuroblastoma breakpoint family, member 1	Unknown
1565875_at	*NUP153*	1.6	2.3E–3	Nucleoporin 153kDa	Unknown
218319_at	*PELI1*	3.0	5.5E–4	Pellino homolog 1 (*Drosophila*)	Unknown
219093_at	*PID1*	–1.8	5.0E–3	Phosphotyrosine interaction domain containing 1	Unknown
1570046_at	*SCRG1*	1.5	2.7E–3	Scrapie responsive protein 1	Unknown
214965_at	*SPATA2L*	1.9	3.3E–3	Spermatogenesis associated 2–like	Unknown
224917_at	*TMEM49*	4.3	4.1E–5	Transmembrane protein 49	Unknown
1561705_at	*TTBK2*	1.6	1.9E–3	Tau tubulin kinase 2	Unknown
233242_at	*WDR73*	1.5	4.8E–3	WD repeat domain 73	Unknown
228280_at	*ZC3HAV1L*	–1.6	4.9E–3	Zinc finger CCCH-type, antiviral 1–like	Unknown
1554007_at	*ZNF483*	–2.4	3.4E–3	Zinc finger protein 483	Unknown

**Fold* denotes fold change between presurgical and postsurgical conditions.

ETJBS

TABLE E12. Quantitative real-time reverse transcriptase polymerase chain reaction target information

Gene symbol	NCBI gene reference	Assay ID	Amplicon length	Context sequence
MEF2C	NM_001131005.1	Hs00231149_m1	101	CAGGCACCAGTGCAGGGAACGGGTA
FBXO32	NM_148177.1	Hs01041408_m1	70	CGGCAGATCCGCAAACGATTAATTC
TRIM63	NM_032588.2	Hs00822397_m1	63–94	TCCCGTCGAGTGACCAAGGAGAACA
CTSL1	NM_145918.2	Hs00377632_m1	85	GAAGAACAGCTGGGGTGAAGAATGG
SOD2	NM_001024465.1	Hs00167309_m1	67	AGGAACAACAGGCCTTATTCCACTG
POLR2A	NM_000937.3	Hs01108291_m1	86	GCTATAAGGTGGAACGGCACATGTG
B2M	NM_004048.2	Hs99999907_m1	75	AGTGGGATCGAGACATGTAAGCAGC

NCBI, National Center for Biotechnology Information.